Some recent contributions to 50 years of EXAFS

Joseph C. Woicik

NIST

Collaborators:

- Cherno Jaye (*SST-1*), Conan Weiland (*SST-2*), Bruce Ravel (*BMM*), and Daniel Fischer (*GL*), *NIST*
- Eric Shirley, Eric Cockayne, and Igor Levin, *NIST*
- Abdul Rumaiz and Milinda Abeykoon, *BNL*
- Joshua Kas and John Rehr, *U. of Washington*
- *Special Mention: A. Broadbent (BNL) & FMB Oxford*

NIST - NSLS-II Beamlines a National User Facility
at Brookhaven National Laboratory

NIST MATERIAL MEASUREMENT LABORATORY

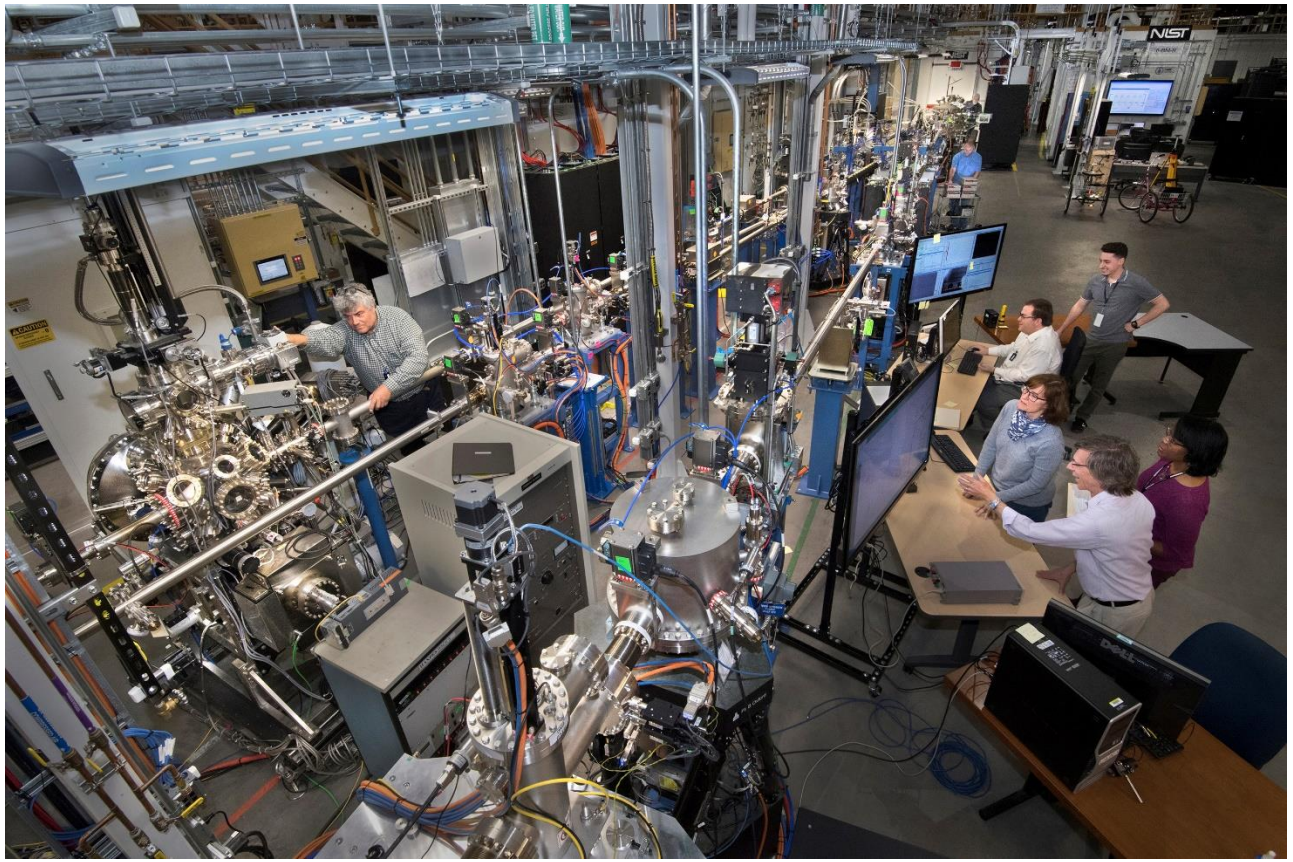

NIST X-ray Spectroscopy Beamlines Soft (R) and Tender (L)
Hard X-ray (R, rear in back)
And some of the Synchrotron Science Group of 12

- ***Reaching full operations in Nov. 2019***, the NIST X-ray beamlines at NSLS-II, probe the structural, chemical, and electronic properties of an unprecedented range of materials.
- Focus on manufacturing relevant environments and collaboration mechanisms that support industrial research and technology transfer.
- CRADAs for collaboration and regular access.
- NIST personnel, stationed at the NSLS-II, supports both NIST priority programs as well as the broader scientific community through the NSLS-II General User Program.

SST-1: 85 eV – 2175 eV
SST-2: 1985 eV – 6500 eV
BMM: 4000 eV – 23.5 keV

Topics:

- Ti 1*s* and Ti 2*p* photoelectron satellite structure of $SrTiO_3$ and TiO_2.
- The “dark” $M_{4,5}$ edges of Au and Pt and the “Zeeman-Auger” effect.
- Lattice vibrations and the d-level chemistry of CuBr.

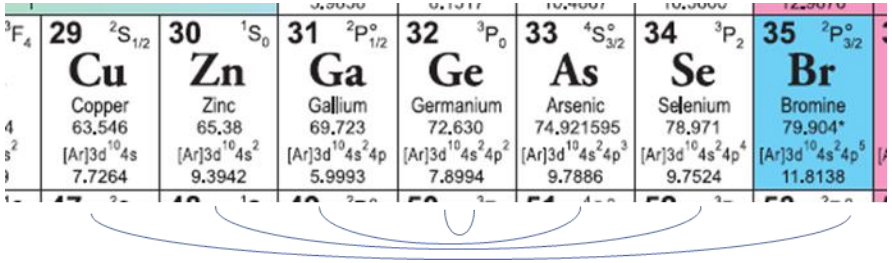

Developments:

- ***Core-hole spectral function.***
- ***Orbital blocking and use of core-hole memory.***
- ***Lattice vibrations and near-edge structure.***

Additional Topics

On the nature of S_0^2 and a quote from Ed.

- AND –

The need for LRO theory of NEXAFS.

Topics:

- Ti 1*s* and Ti 2*p* photoelectron satellite structure of $SrTiO_3$ and TiO_2.
- The “dark” $M_{4,5}$ edges of Au and Pt and the “Zeeman-Auger” effect.
- Lattice vibrations and the d-level chemistry of CuBr.

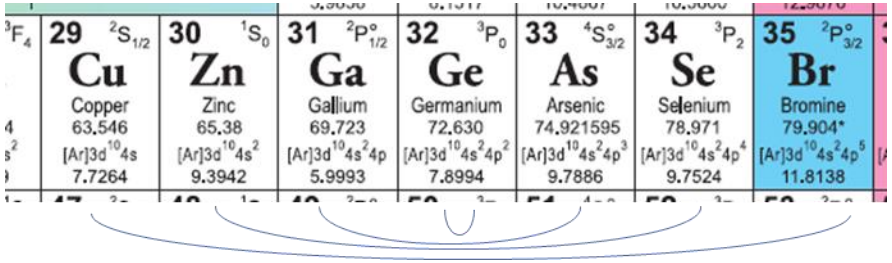

Ab initio RT-TDDFT cumulant core hole Green's function TiO_2

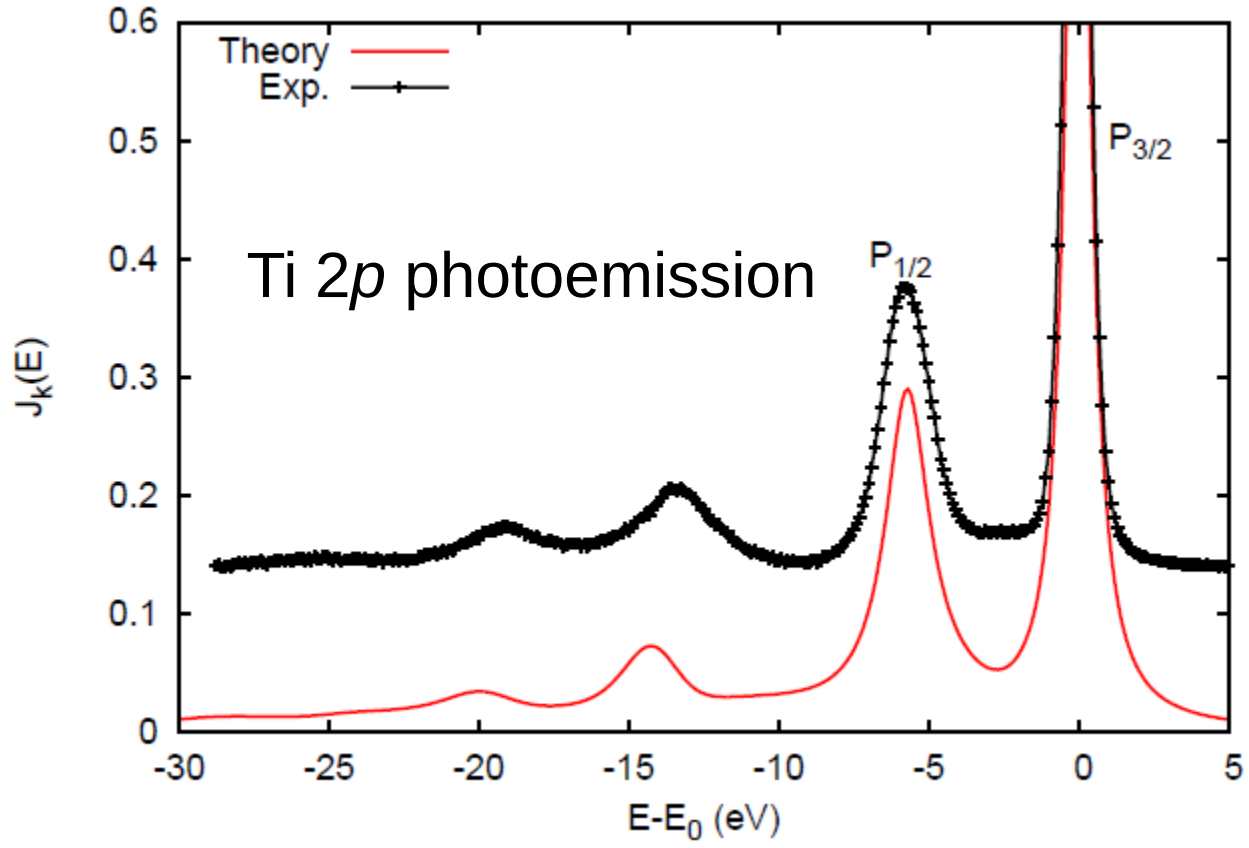

J.J. Kas et al., *Phys. Rev. B* **91**, 121112(R) (2015).

Configuration interaction cluster model "analysis"

$$|d^n\rangle,$$

$$|d^{n+1}\underline{L}\rangle = \frac{1}{\sqrt{10-n}} \sum_{\mu} d^{\dagger}_{\mu} p_{\mu} |d^n\rangle,$$

$$|d^{n+2}\underline{L}^2\rangle = \sqrt{\frac{2}{(10-n)(9-n)}} \sum_{\substack{\mu,\mu' \\ \mu \neq \mu'}} d^{\dagger}_{\mu} d^{\dagger}_{\mu'} p_{\mu} p_{\mu'} |d^n\rangle,$$

U: On-site *d*-*d* Coulomb repulsion energy
Δ: Charge-transfer energy
T: Ligand *p*-metal *d* hybridization energy

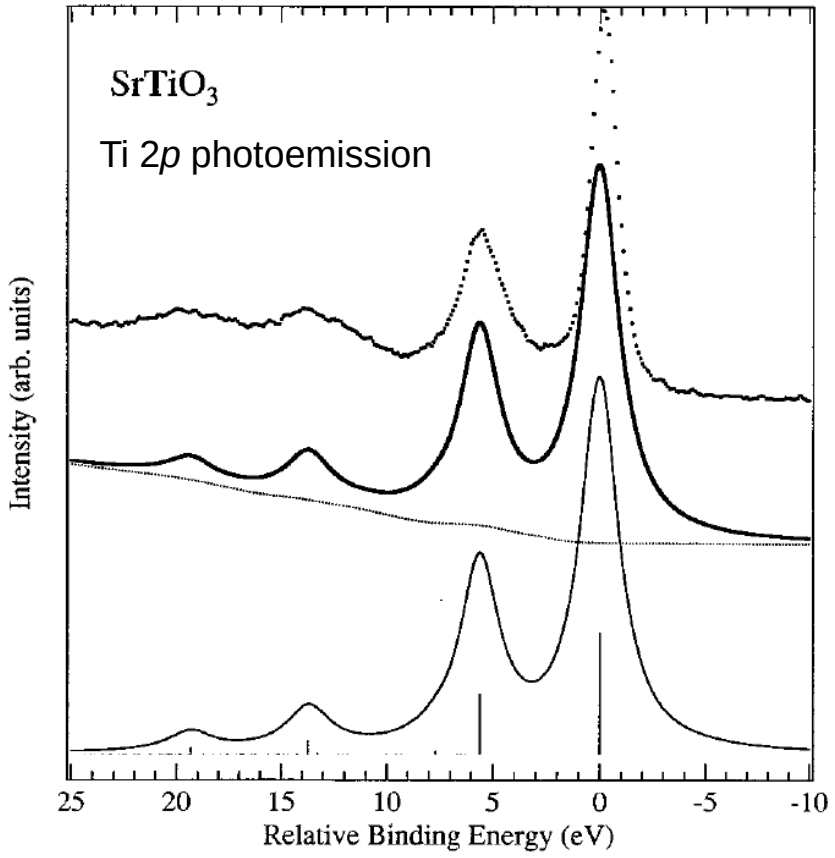

A.E. Bocquet et al., *Phys. Rev. B* **53**, 1161 (1996).

Ti 2*p* photoemission core line $SrTiO_3$

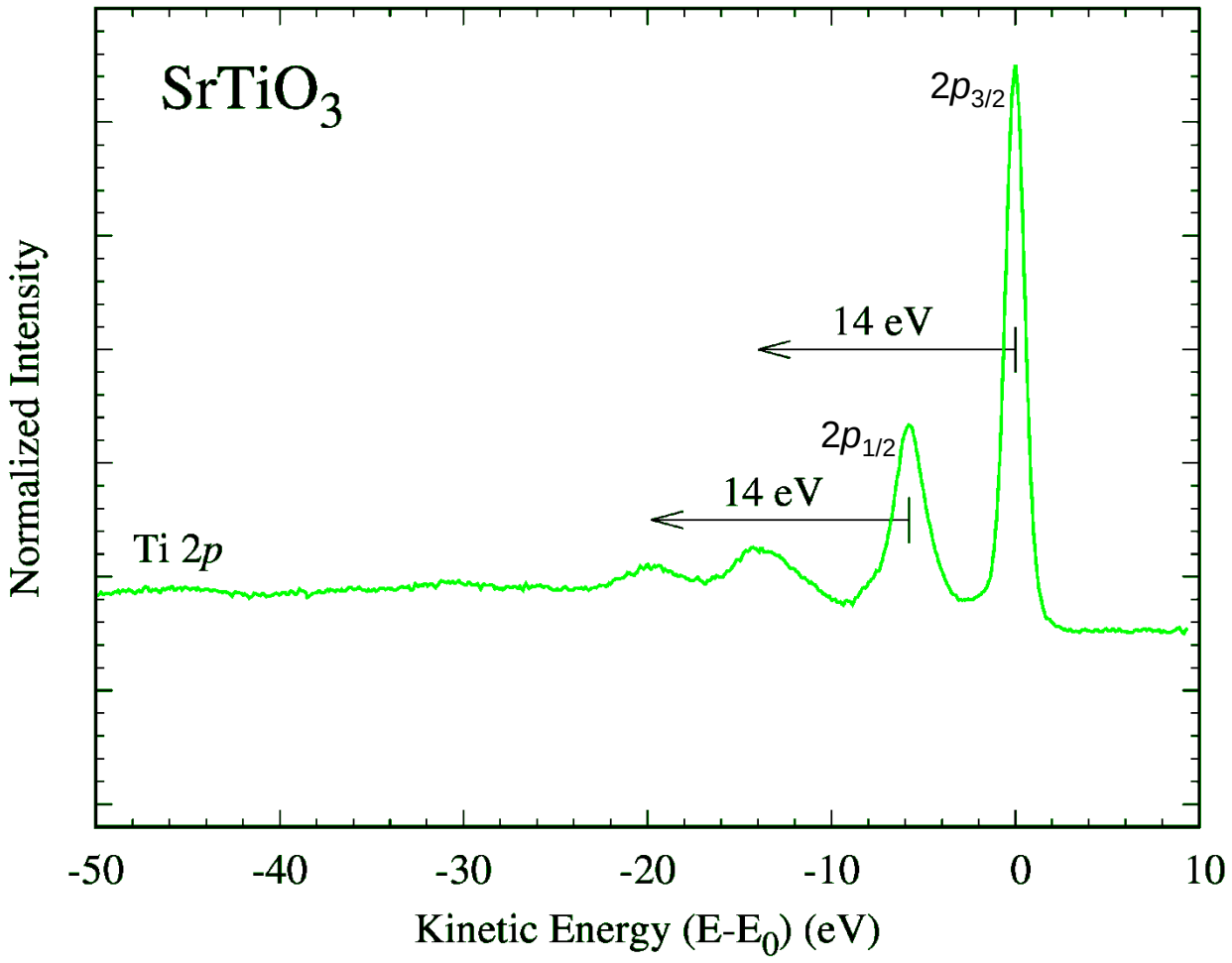

- *Likely* most studied core line after Si 2*p* ....

Ti 1*s* and 2*p* photoemission core lines $SrTiO_3$

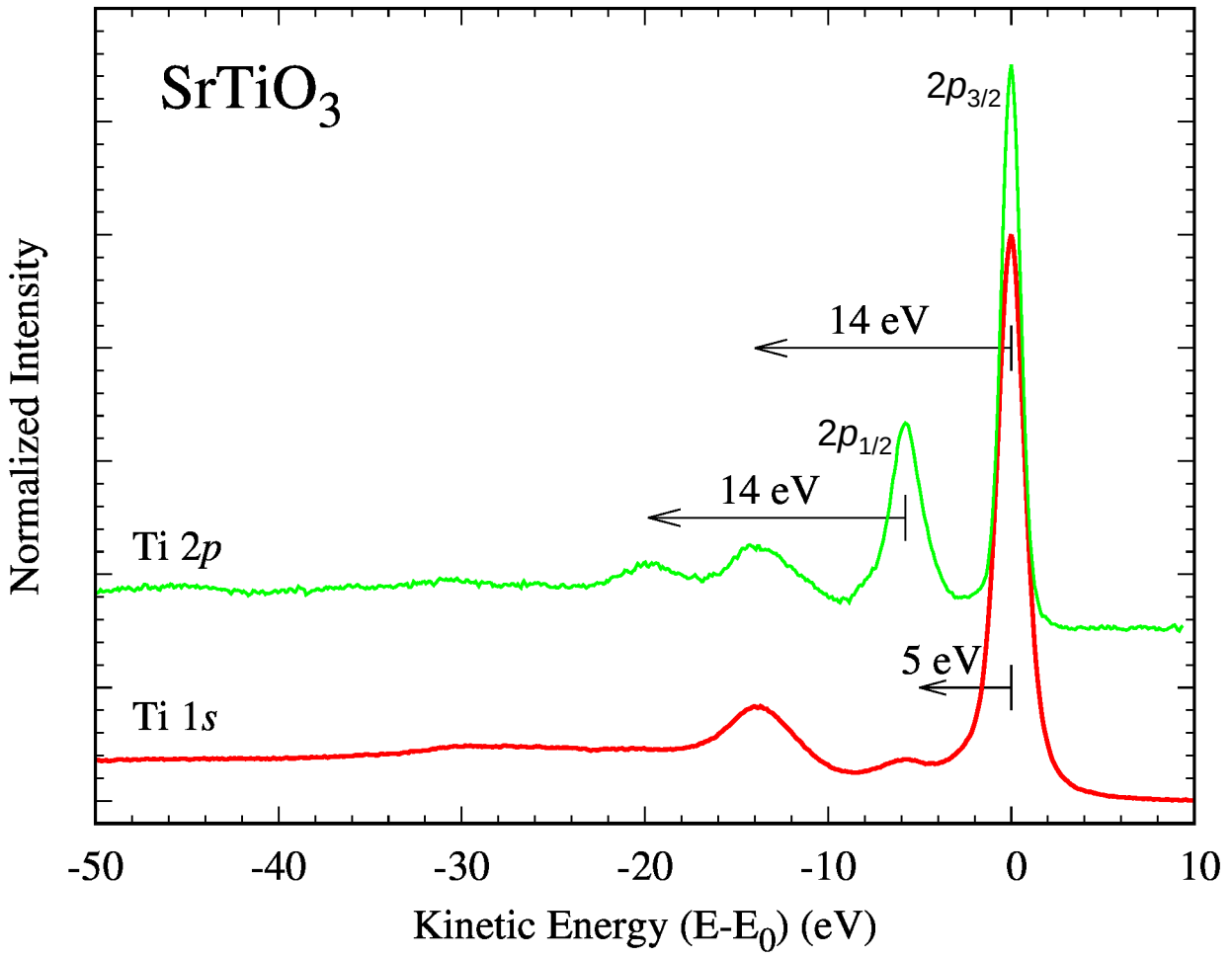

"New" 5 eV Satellite!

Ti 1s photoelectron satellite structure of $SrTiO_3$ and TiO_2

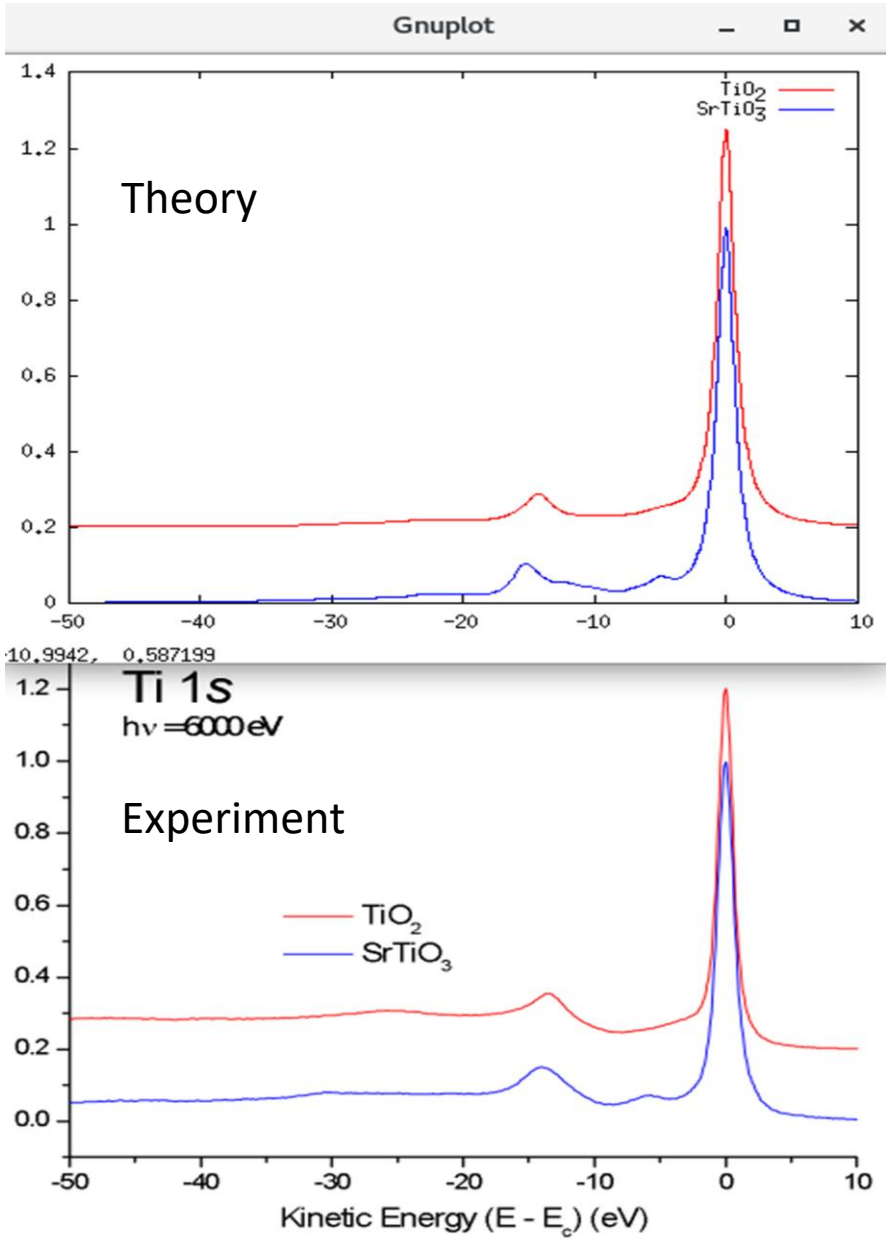

- $SrTiO_3$: O_h
- TiO_2: D_{4h}

Excitation Charge Density $SrTiO_3$

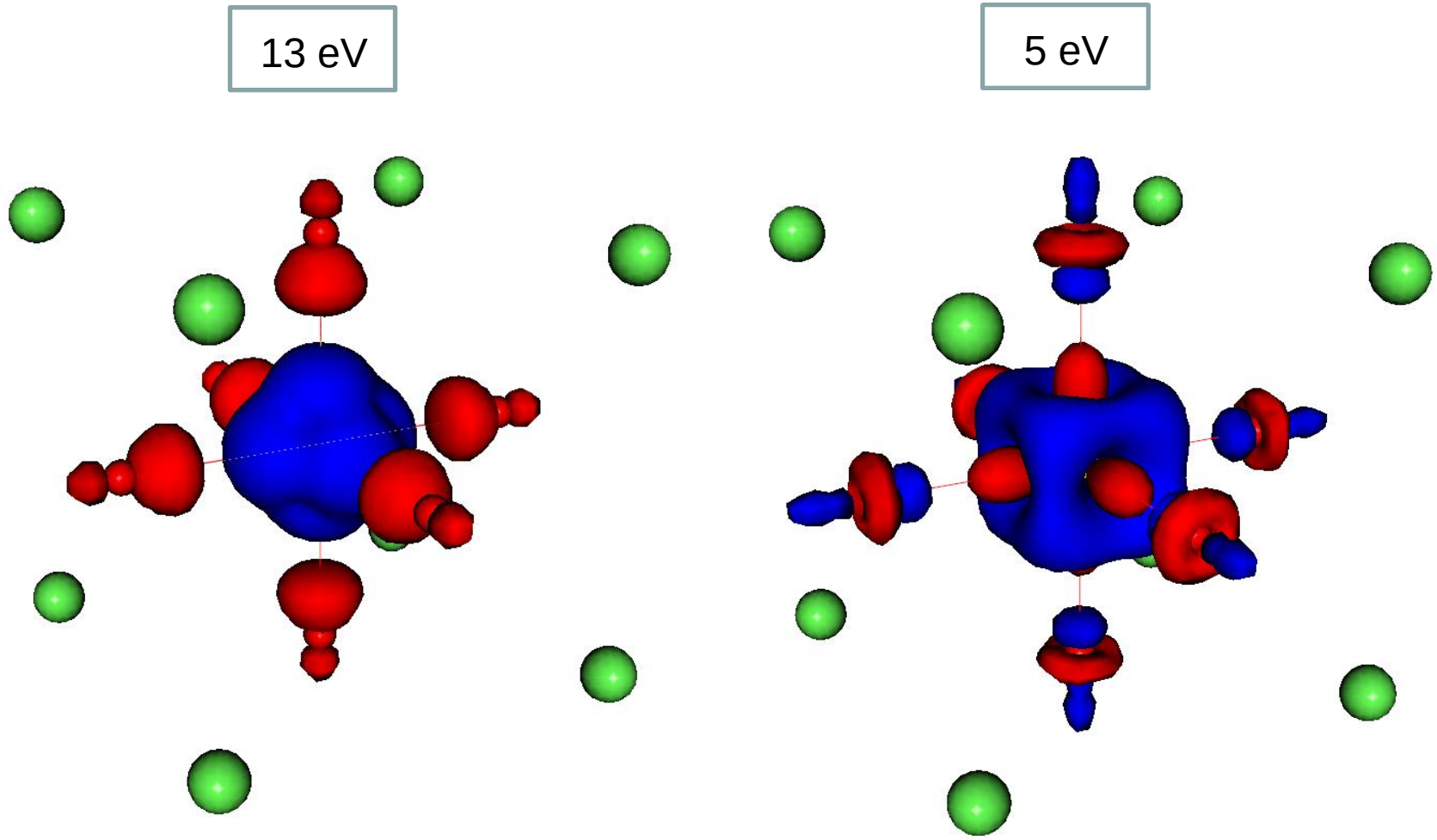

- e_g excitation higher energy *and* larger cross section than t_{2g} excitation …

Core Hole Spectral Function: $L_{2,3}$ XAS

$$\mu(\omega) = \int d\omega' A(\omega, \omega')\mu'(\omega - \omega')$$

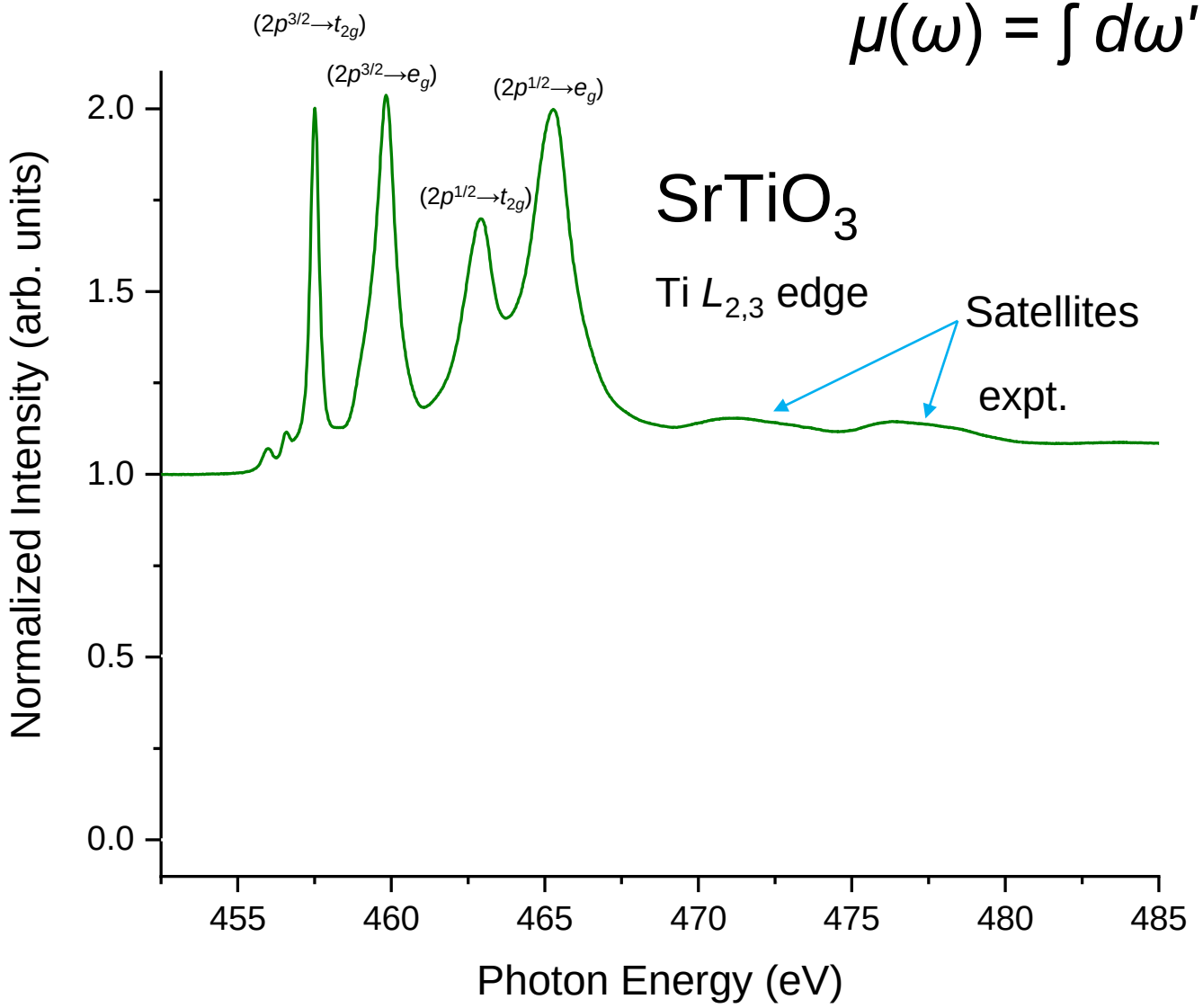

Core Hole Spectral Function: $L_{2,3}$ XAS

$$\mu(\omega) = \int d\omega' A(\omega, \omega')\mu'(\omega - \omega')$$

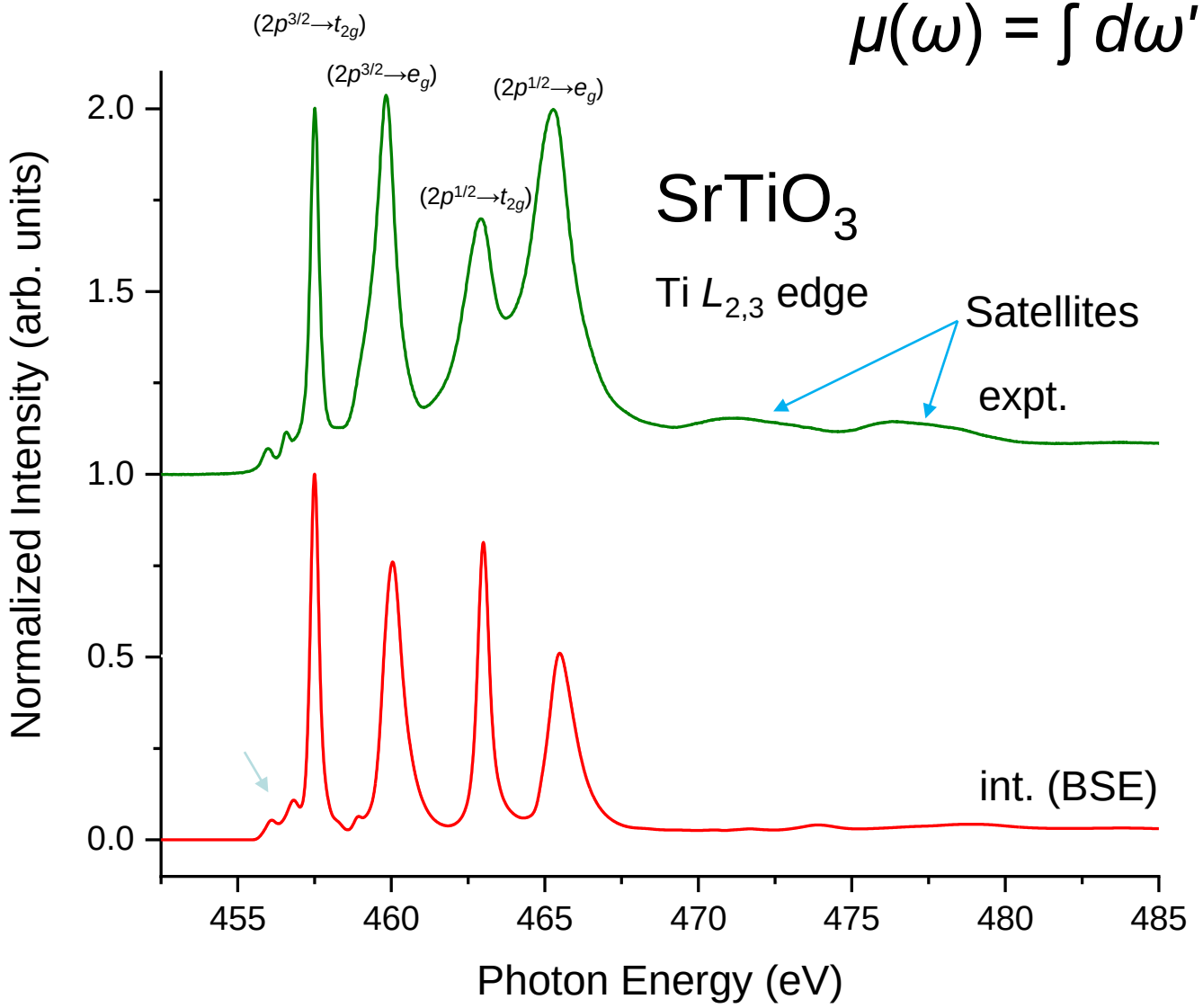

- Multiplets but no multi-electron excitations …

Core Hole Spectral Function: $L_{2,3}$ XAS

$$\mu(\omega) = \int d\omega' A(\omega, \omega')\mu'(\omega - \omega')$$

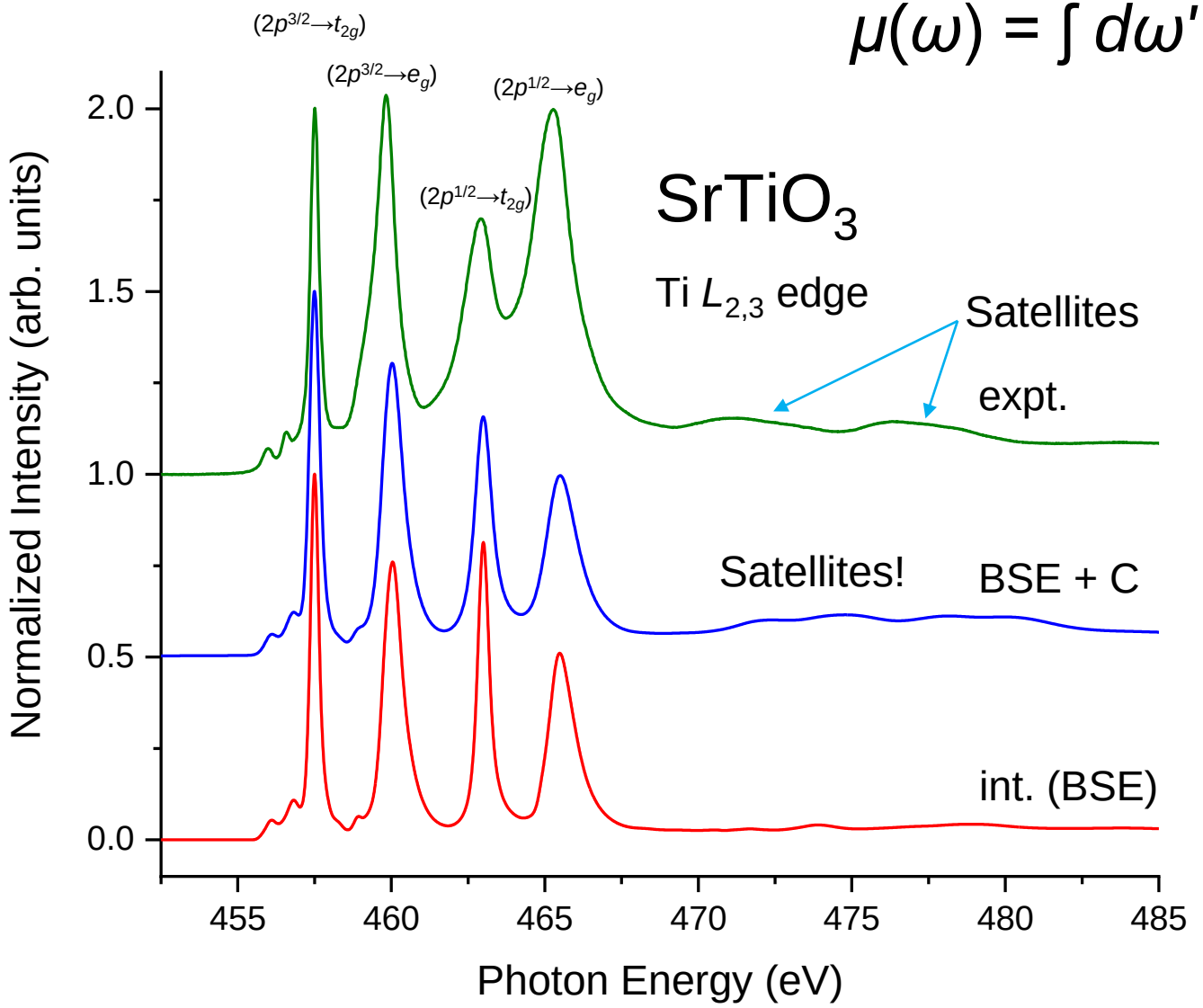

- Satellites are also crystal-field split …

Core Hole Spectral Function: $L_{2,3}$ XAS

$$\mu(\omega) = \int d\omega' A(\omega, \omega')\mu'(\omega - \omega')$$

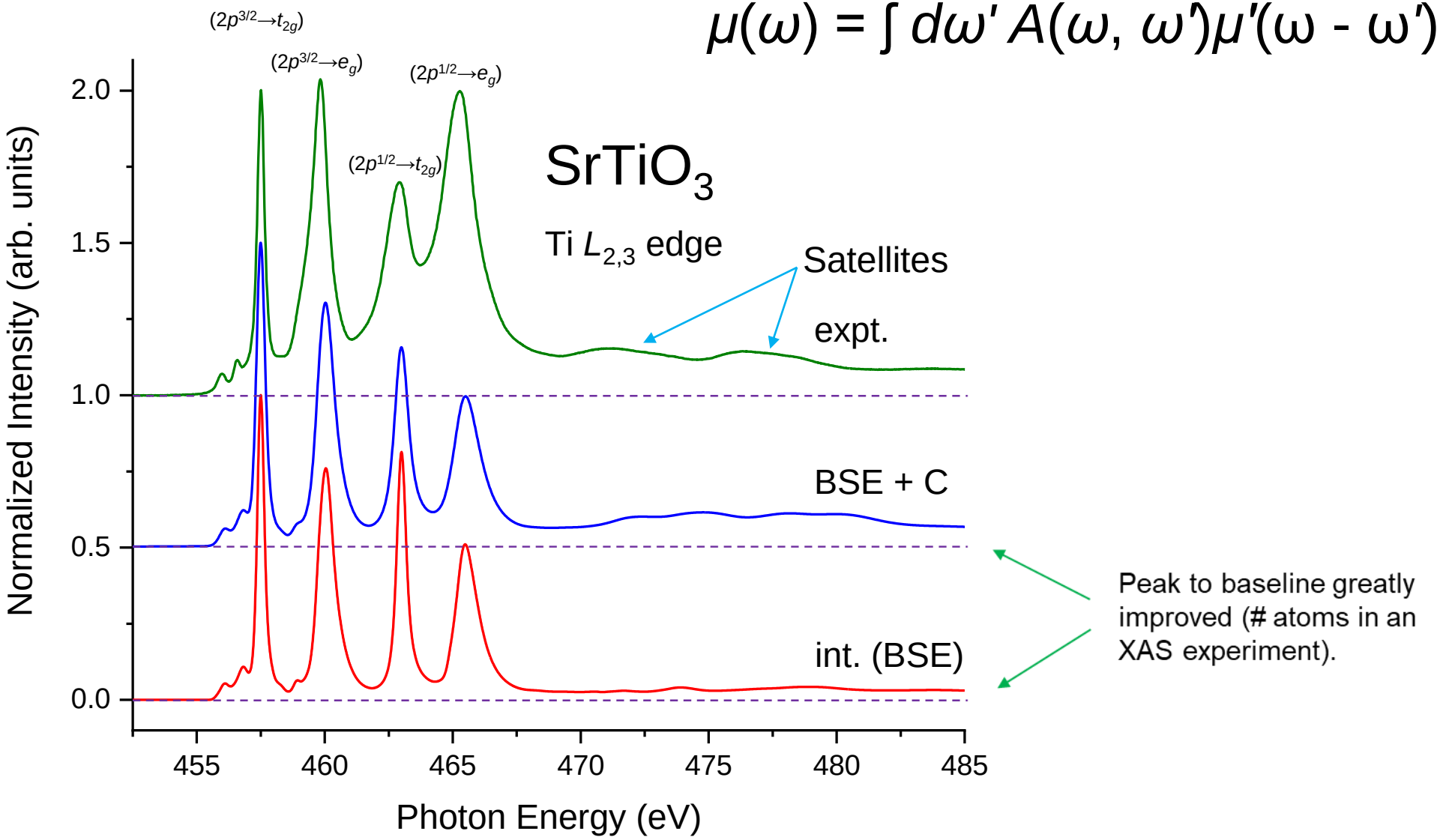

Topics:

✓Ti 1*s* and Ti 2*p* photoelectron satellite structure of $SrTiO_3$ and TiO_2.

- The “dark” $M_{4,5}$ edges of Au and Pt and the “Zeeman-Auger” effect.
- Lattice vibrations and the d-level chemistry of CuBr.

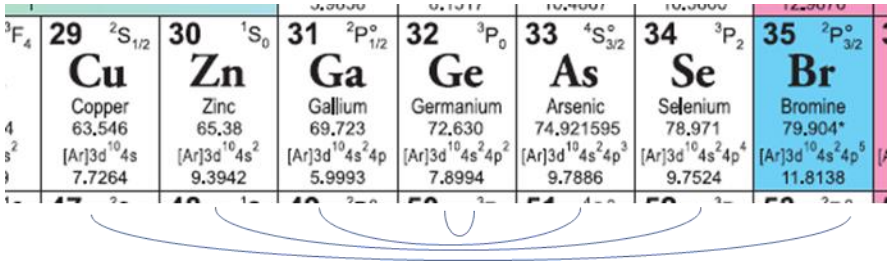

Au and Pt M_5 "Dark" Edges

- Au: 2206 eV
- Pt: 2122 eV

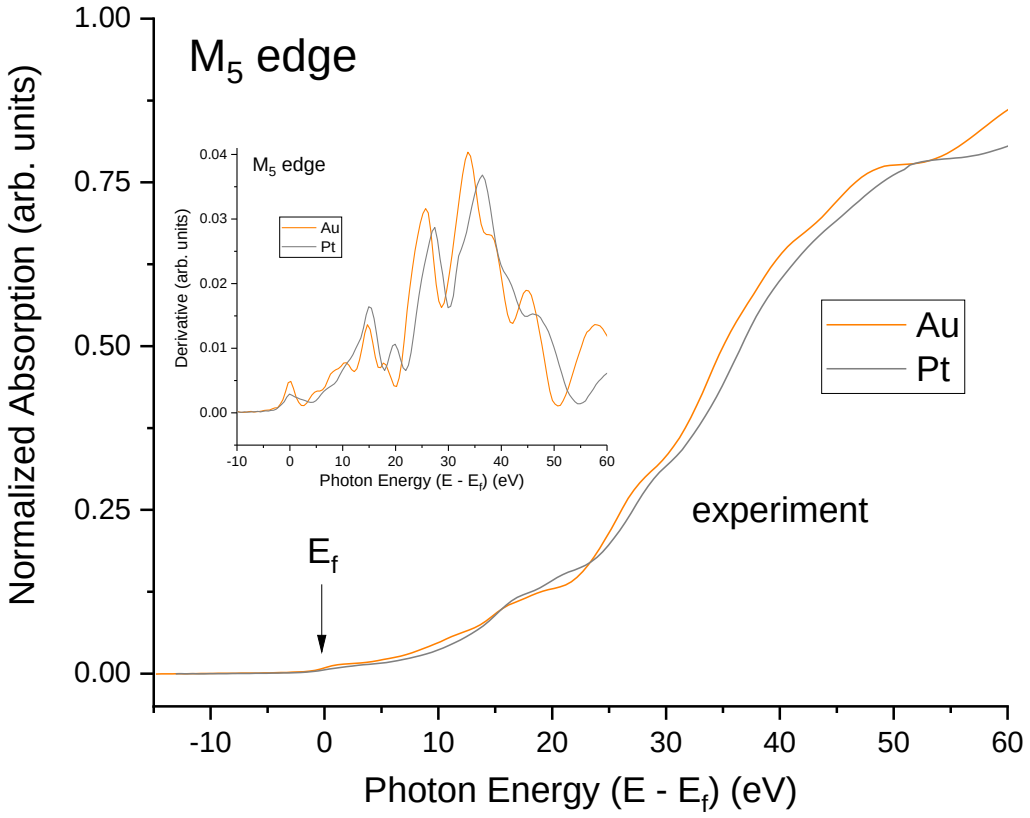

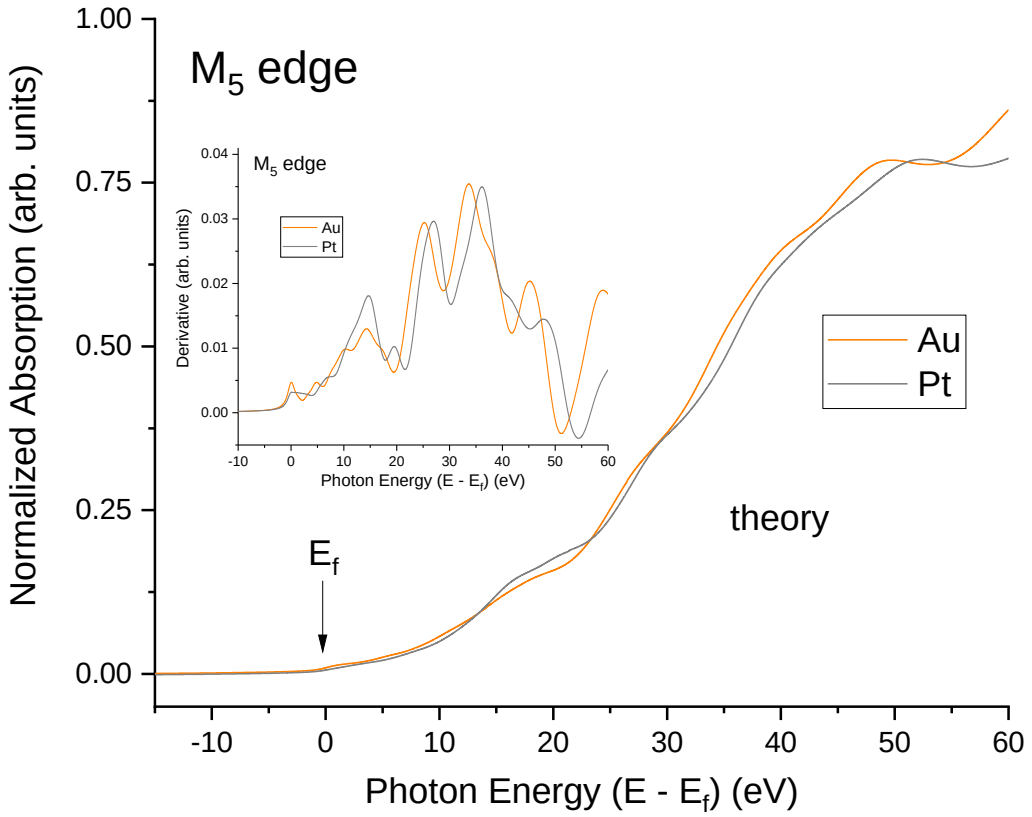

- "Dark" versus "White" line ...

Dark Au and Pt $M_{4,5}$ Edges

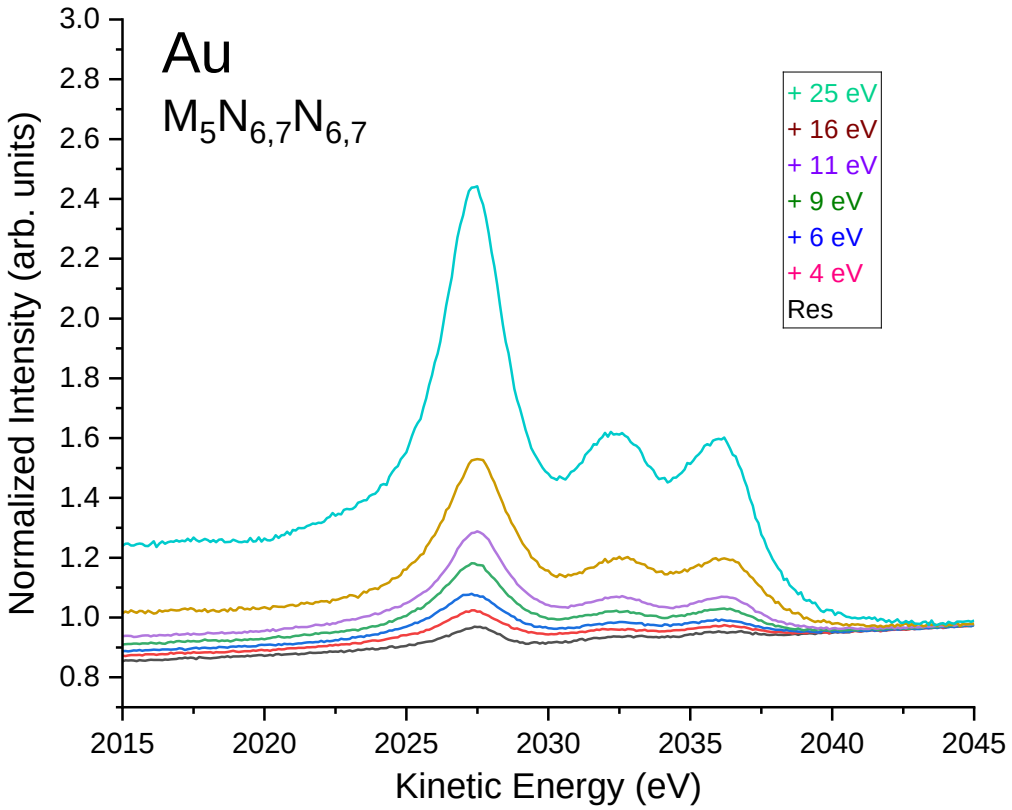

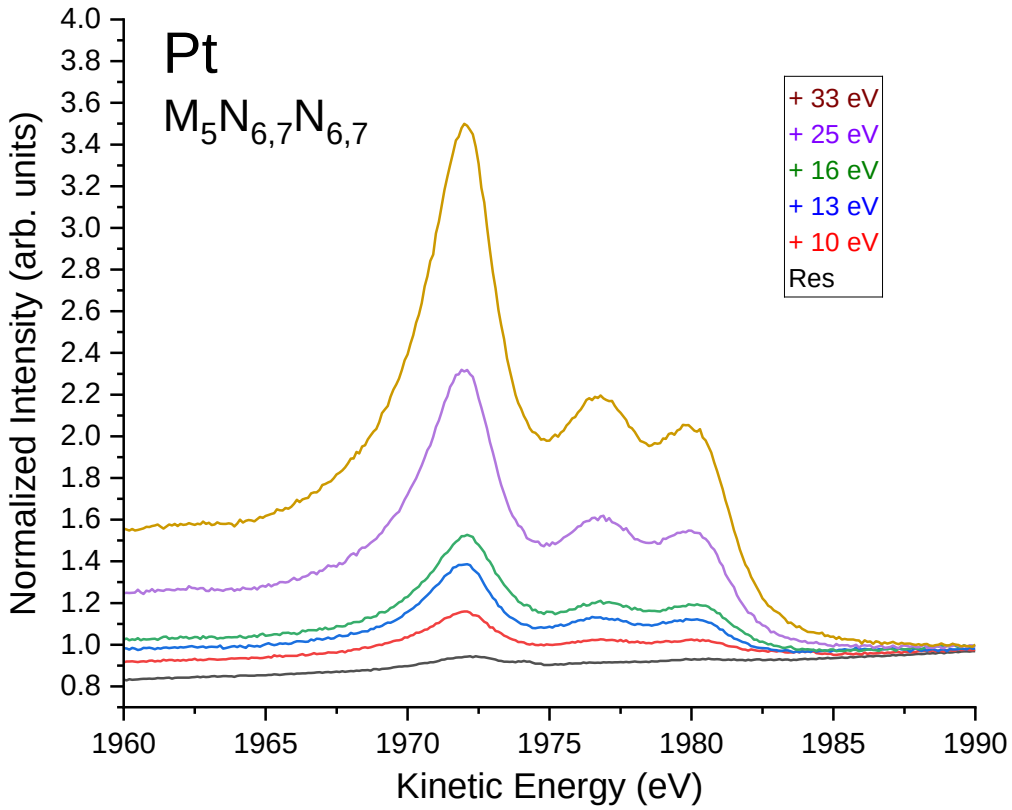

- Identification of E_f from appearance of near-zero Auger intensity at resonance …

Why Dark? Centrifugal Barrier in QM

- $H\Psi = E\Psi$
- $V(\boldsymbol{r}) = V(r) \quad (V(r) = -Ze^2/r)$
- $\Psi(r,\theta,\phi) = R_{nl}(r)\, Y_{lm}(\theta,\phi)$

$$V_{eff}(r) = V(r) + l(l+1)/2m_e r^2$$

- Repulsive potential: States with larger angular momentum (l) extend further from the nucleus ...

Centrifugal Barrier: Au N and O core lines

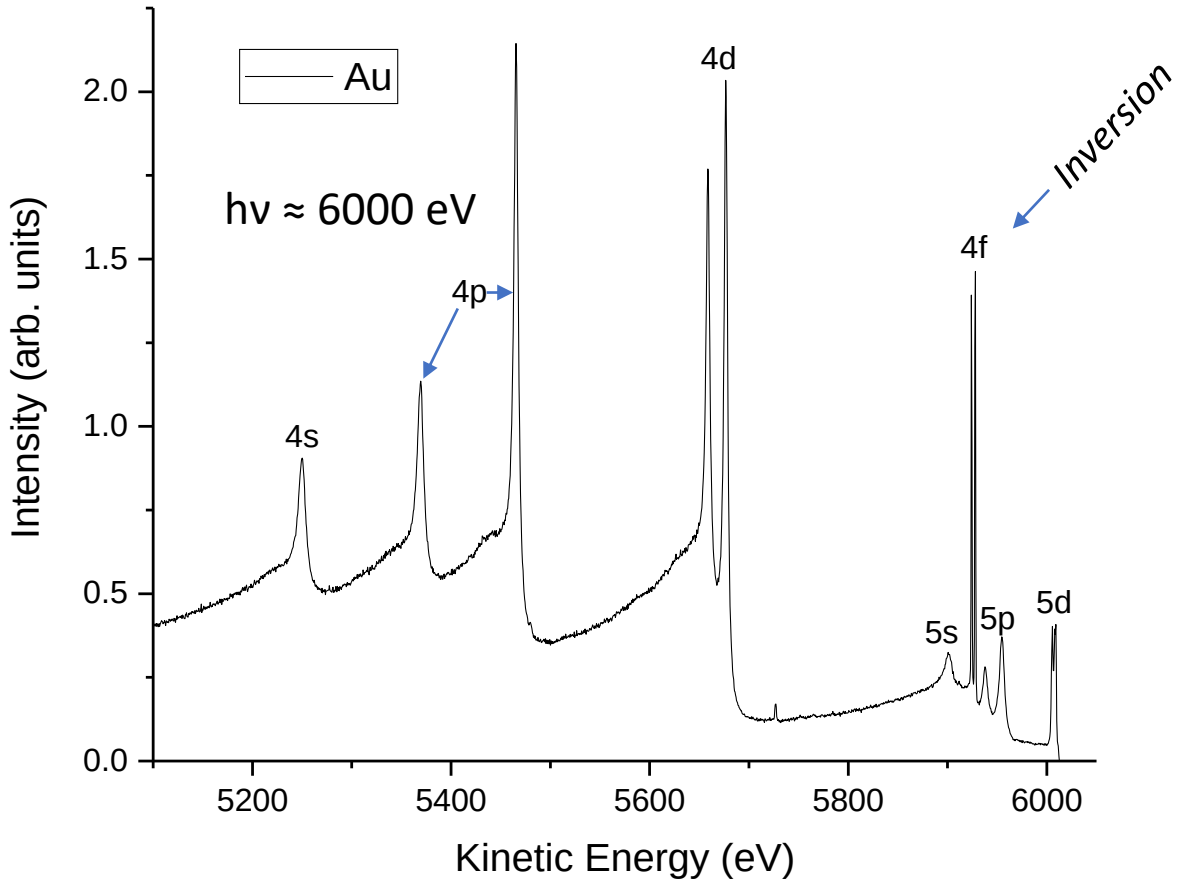

- $E = E_{n,l}$ due to screening for multi-electron atom; i.e., nuclear penetration is greater for states with smaller angular momentum.
- Not in single-electron atom: $E = E_n$.
- S.O.S. also function of l.

$$V_{eff} = V(r) + l(l+1)/2m_e r^2$$

DFT Density of States

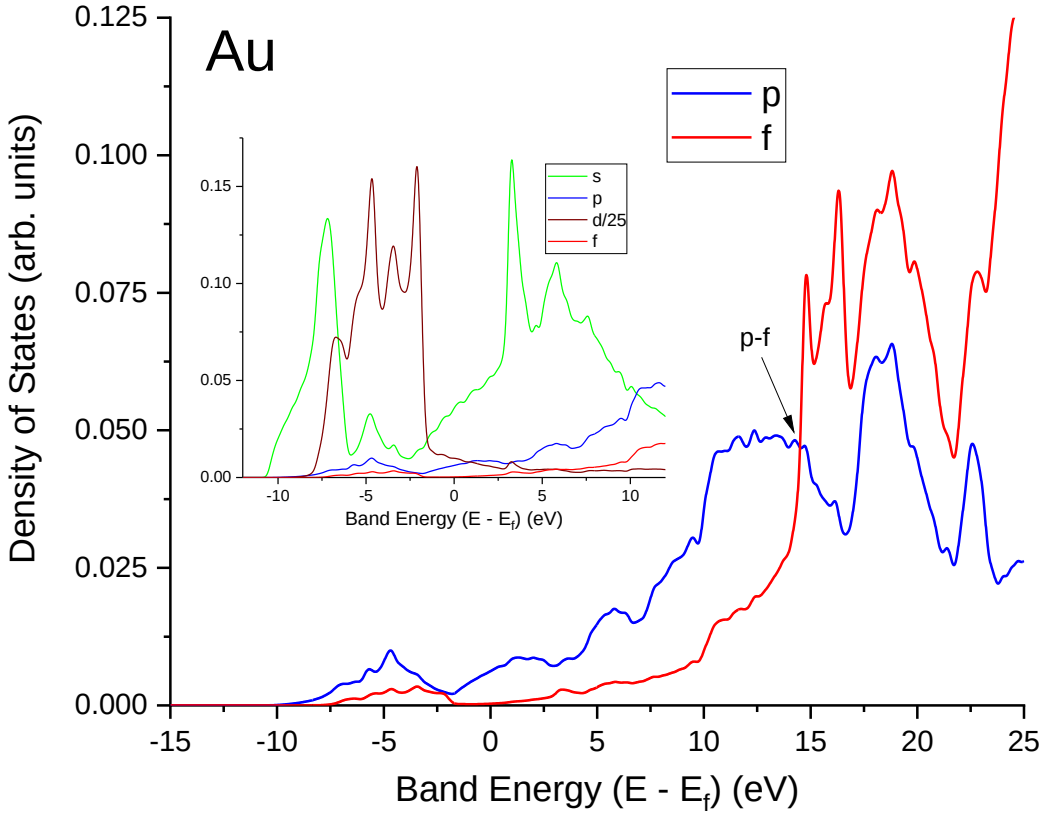

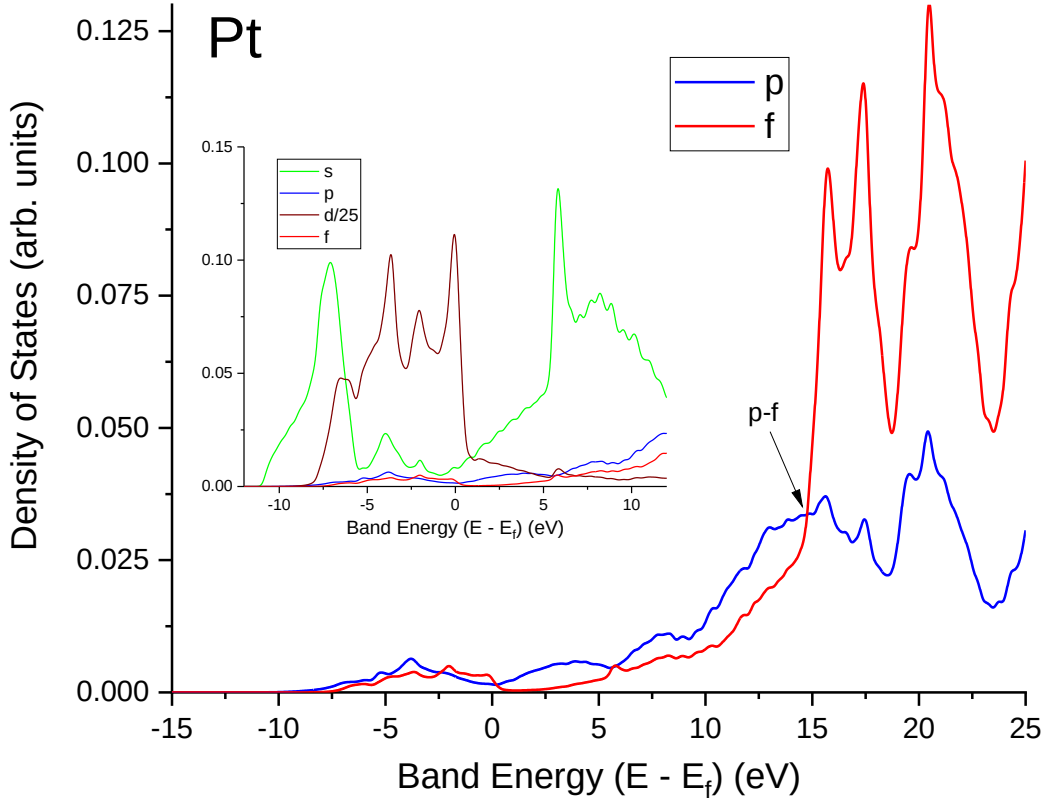

- *d* photoelectron can go out either as a *p* wave or an *f* wave …
- $6p \rightarrow 5f$ crossover in unoccupied states occurs ≈ 15 eV above E_f …
- $(2l+1)_f / (2l+1)_p = 7/3$
- "Dark" because of small *p* density of states at E_f …

Photon Energy Dependence of Au and Pt $M_5N_{6,7}N_{6,7}$ Auger

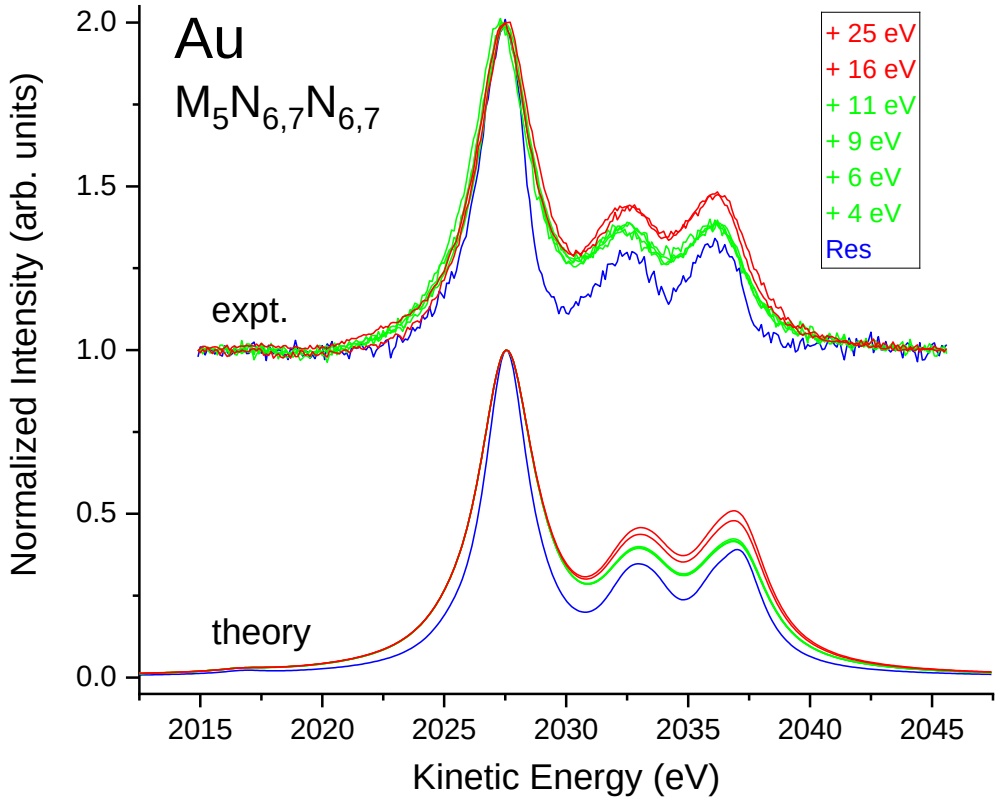

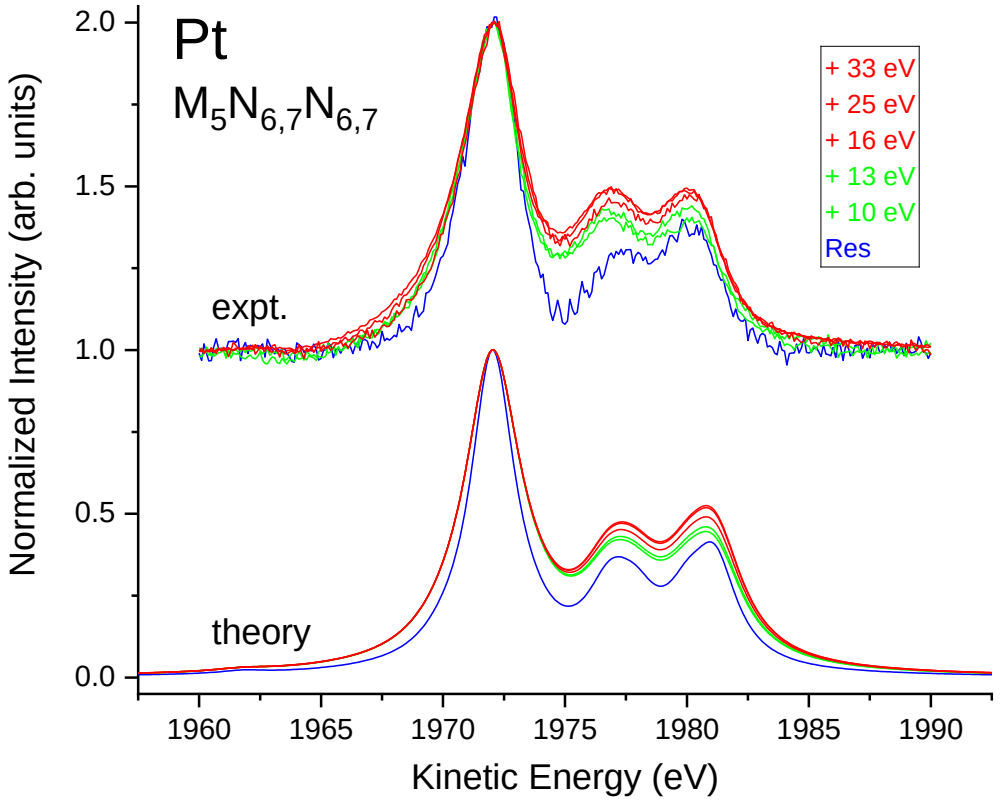

- Anomalous (*discrete*) Auger behavior, especially for “non-interacting” systems …

Dipole Selection Rules and Orbital Blocking

- $< \psi_f \mid \boldsymbol{\epsilon} \cdot \boldsymbol{r} \mid \psi_i >$
- $\boldsymbol{\epsilon} \,//\, \boldsymbol{z}$
- $\boldsymbol{\epsilon} \cdot \boldsymbol{r} \,\alpha\, Y_{1,0}(\theta,\phi)$

$M_{4,5} = 3d$

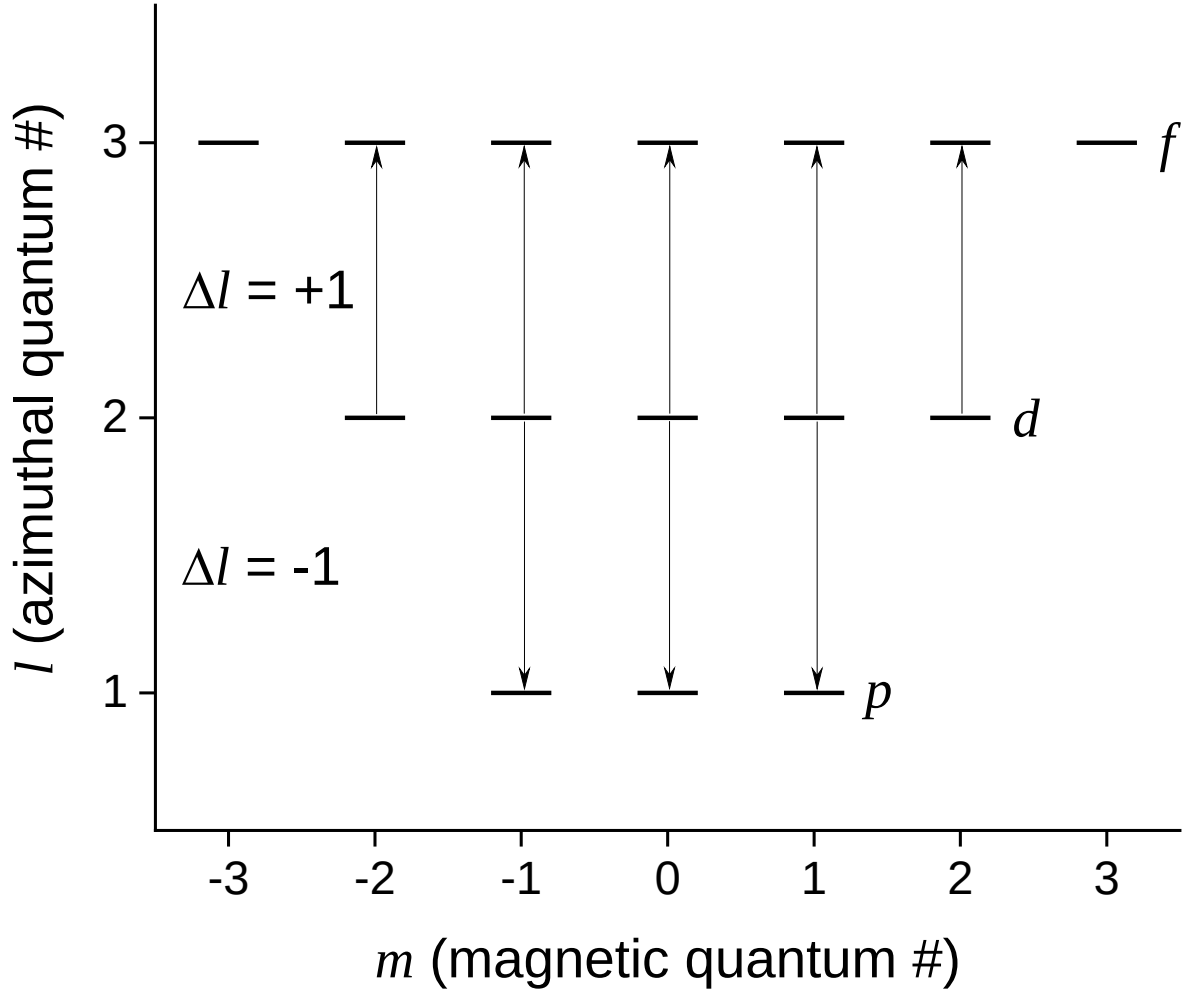

$< Y_{lf,mf} \mid Y_{1,0} \mid Y_{li,mi} >$

- $\Delta m = 0$
- $\Delta l = \pm 1$

Dipole Selection Rules and Orbital Blocking

- $< \psi_f \mid \boldsymbol{\epsilon} \cdot \boldsymbol{r} \mid \psi_i >$
- $\boldsymbol{\epsilon} \,//\, \boldsymbol{z}$
- $\boldsymbol{\epsilon} \cdot \boldsymbol{r} \, \alpha \, Y_{1,0}(\theta,\phi)$

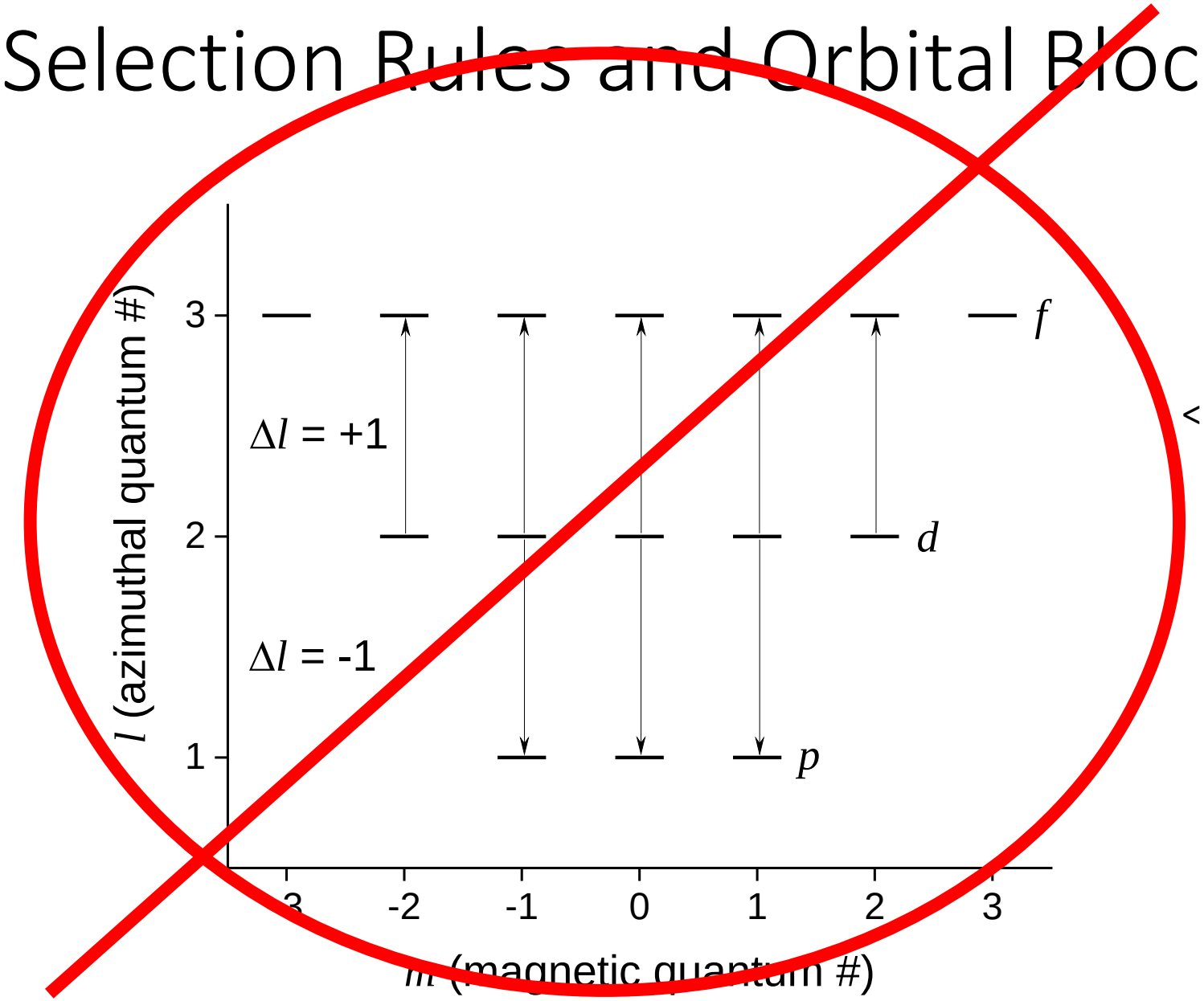

$< Y_{lf,mf} \mid Y_{1,0} \mid Y_{li,mi} >$

- $\Delta m = 0$
- $\Delta l = \pm 1$

Zeeman Diagram for $M_{4,5}$ edge XAS

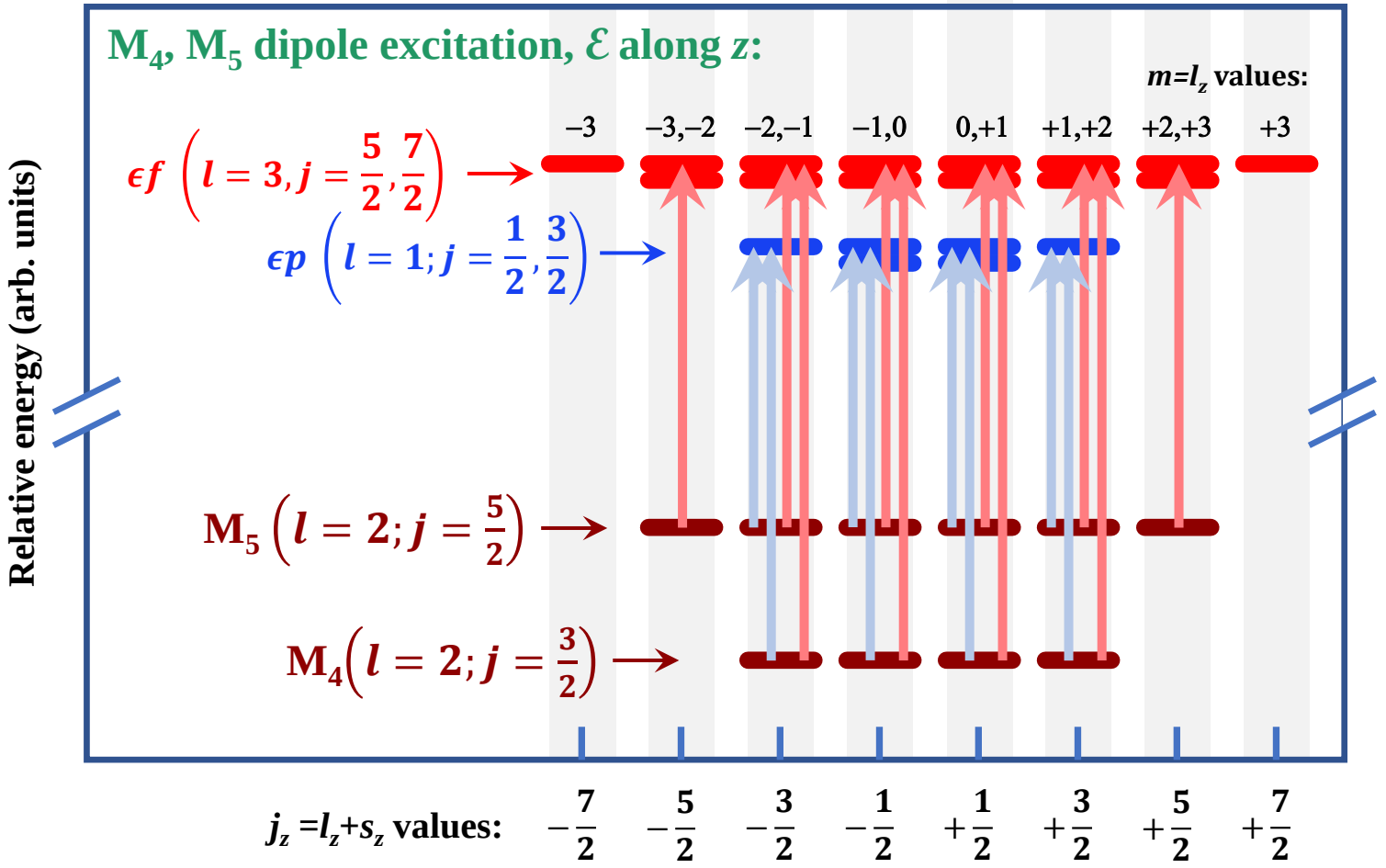

- l_z
- $j_z = l_z + s_z$

j_z dependence of Auger basis functions for $M_{4,5}$ core holes

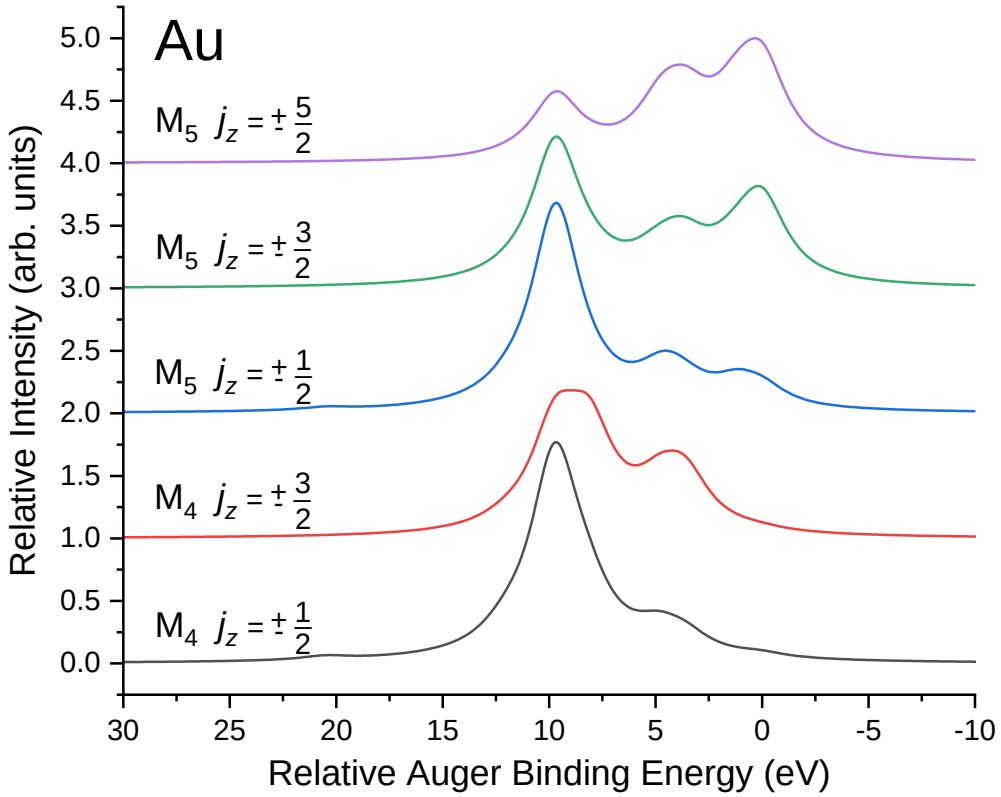

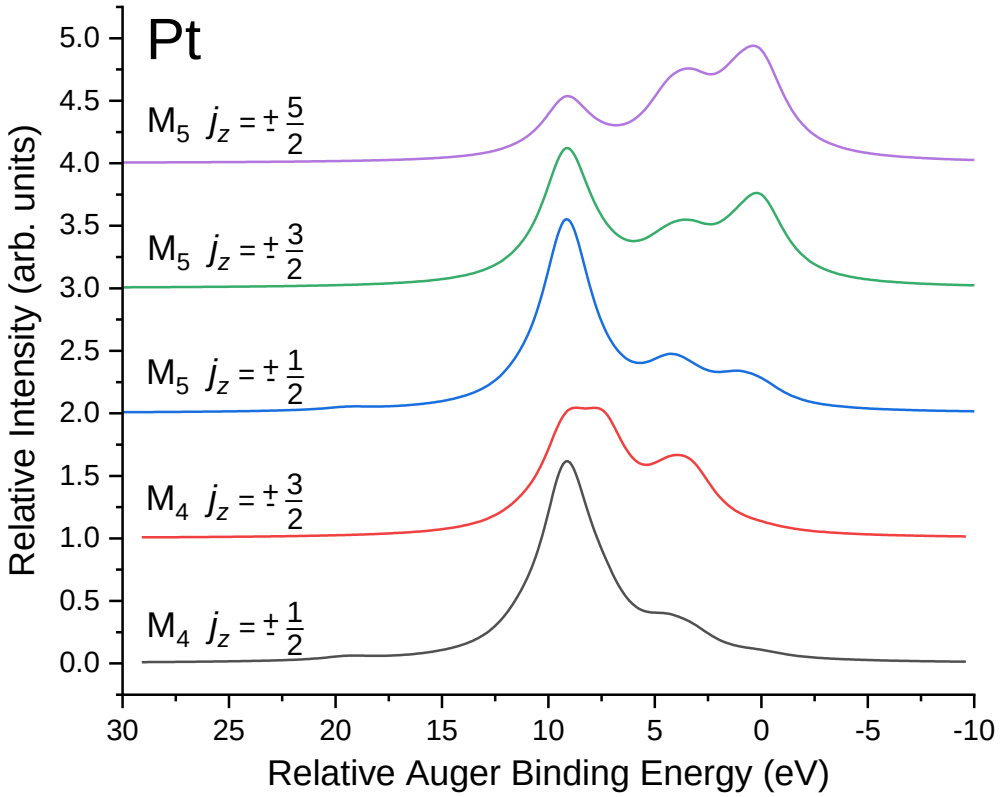

- $j_z = l_z + s_z$

Photon Energy Dependence of Au and Pt $M_5N_{6,7}N_{6,7}$ Auger

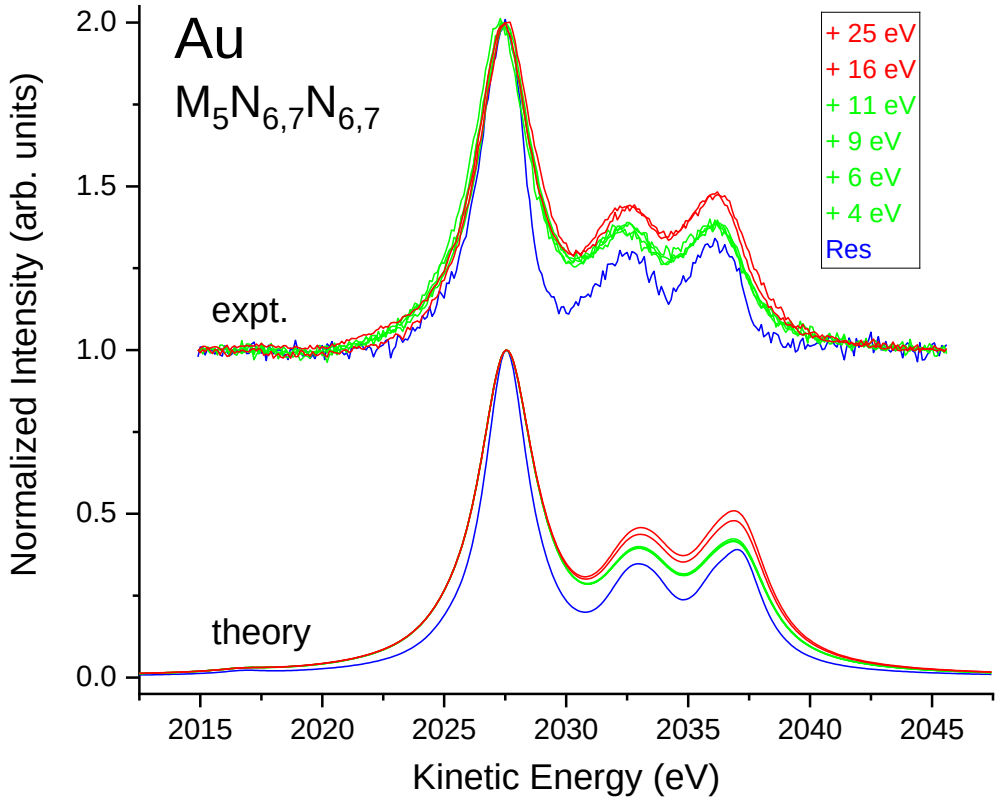

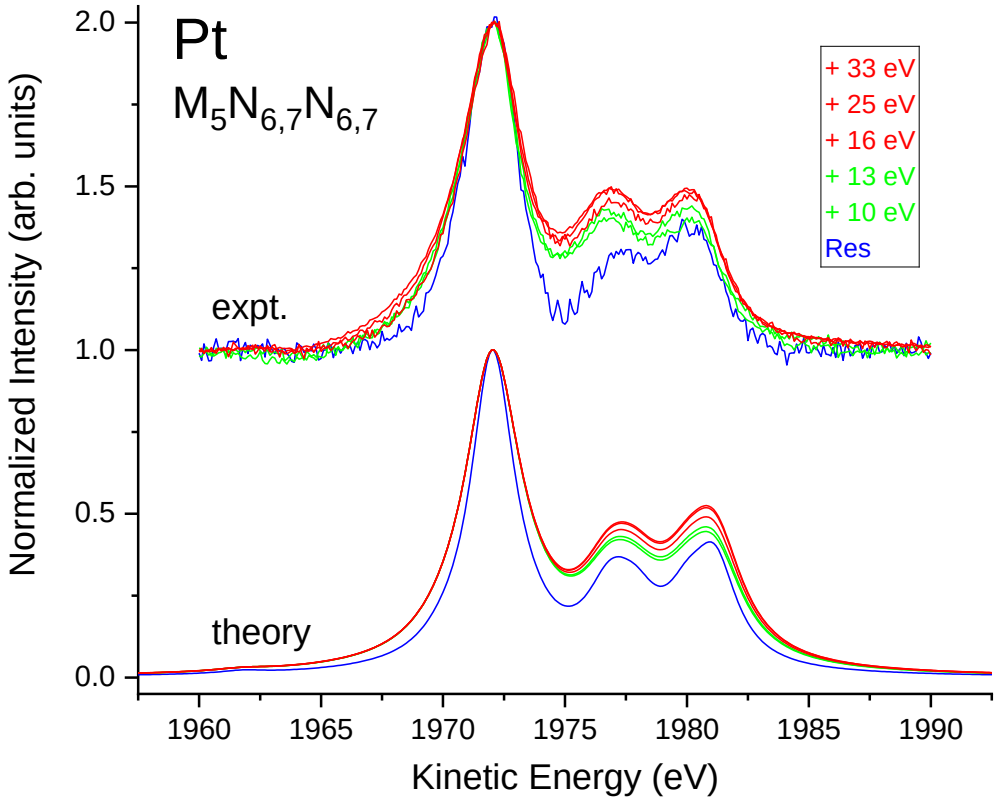

- Core hole retains memory of how it was created throughout its Auger decay …

Au and Pt $M_4N_{6,7}N_{6,7}$ Auger

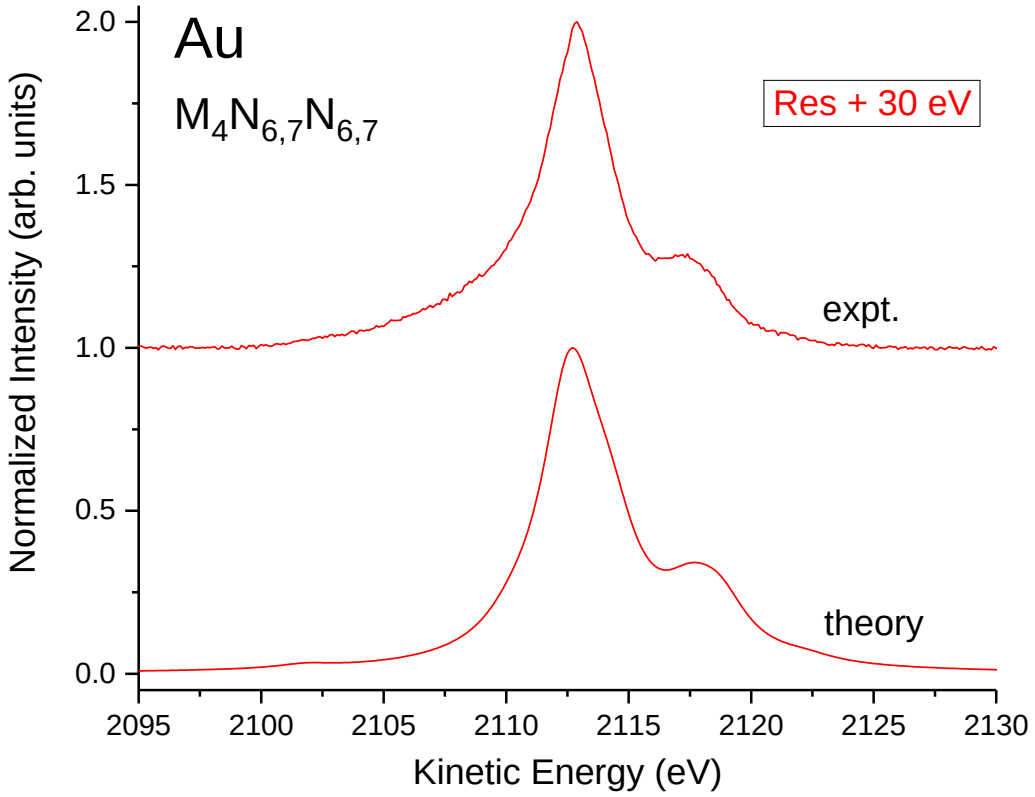

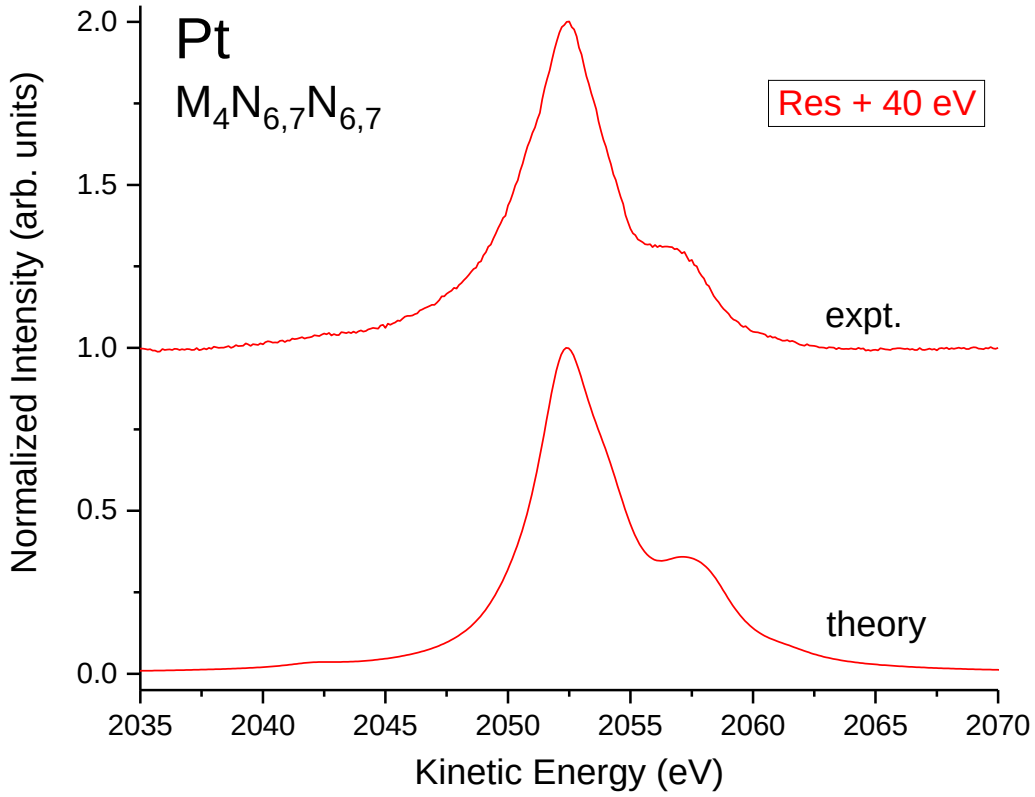

- Effect of different initial core-hole j_z states …

Ag L_3 XAS and L_3-$M_{4,5}M_{4,5}$ Auger Decay

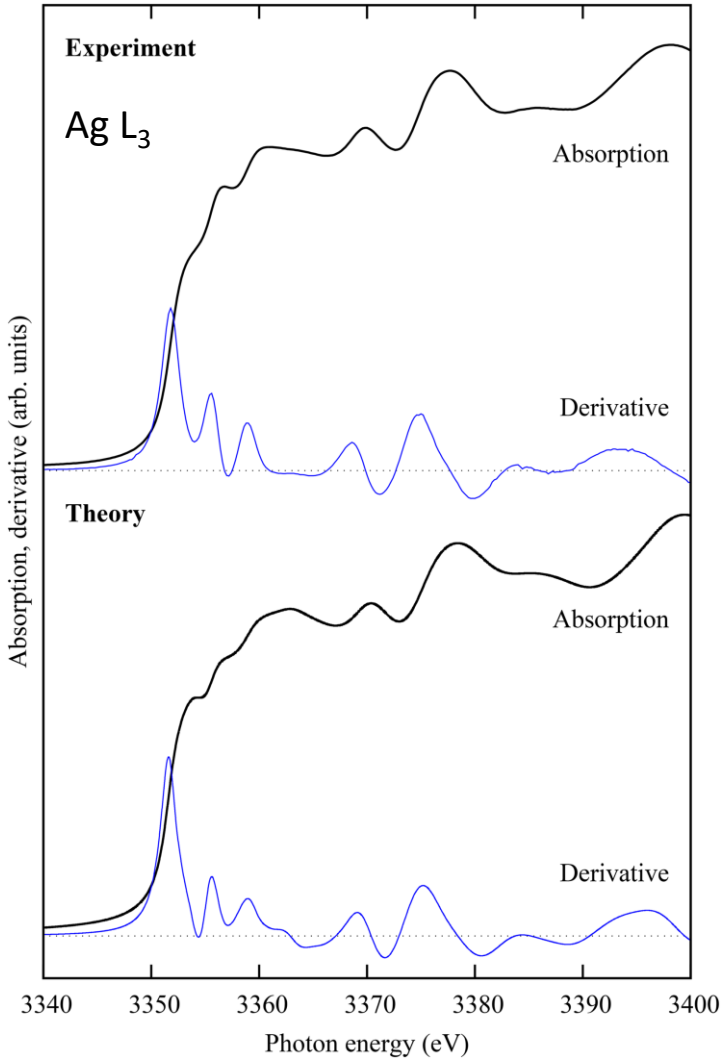

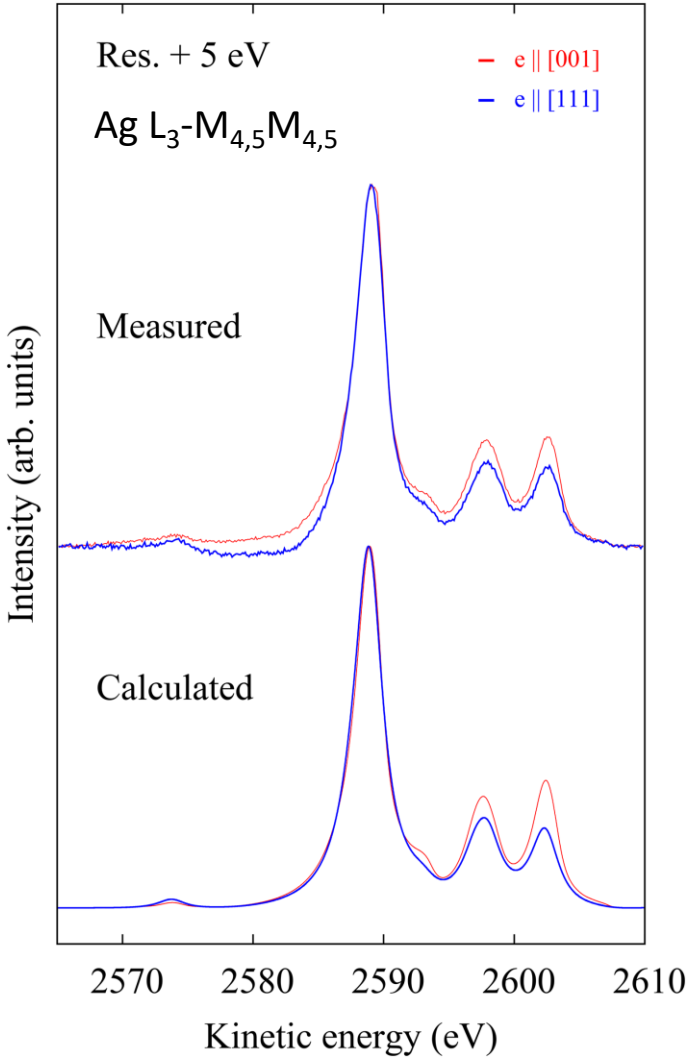

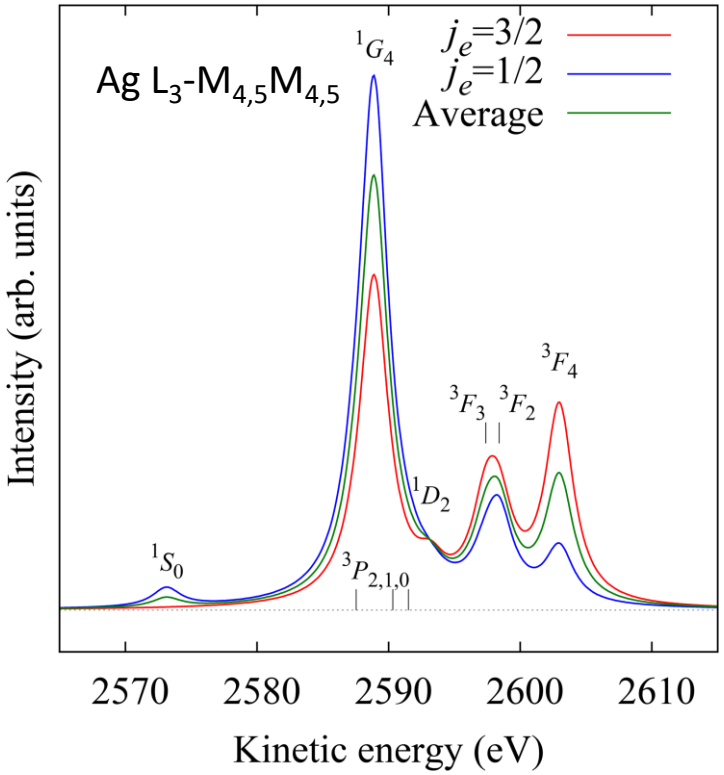

- Ag single crystal

E.L. Shirley, C. Weiland, and J.C. Woicik, *J. Vac. Sci. Technol. A* **40**, 023410 (2022):

"Commemorating the Career of David Arthur Shirley."

Partial DOS: Use of Core Hole Memory

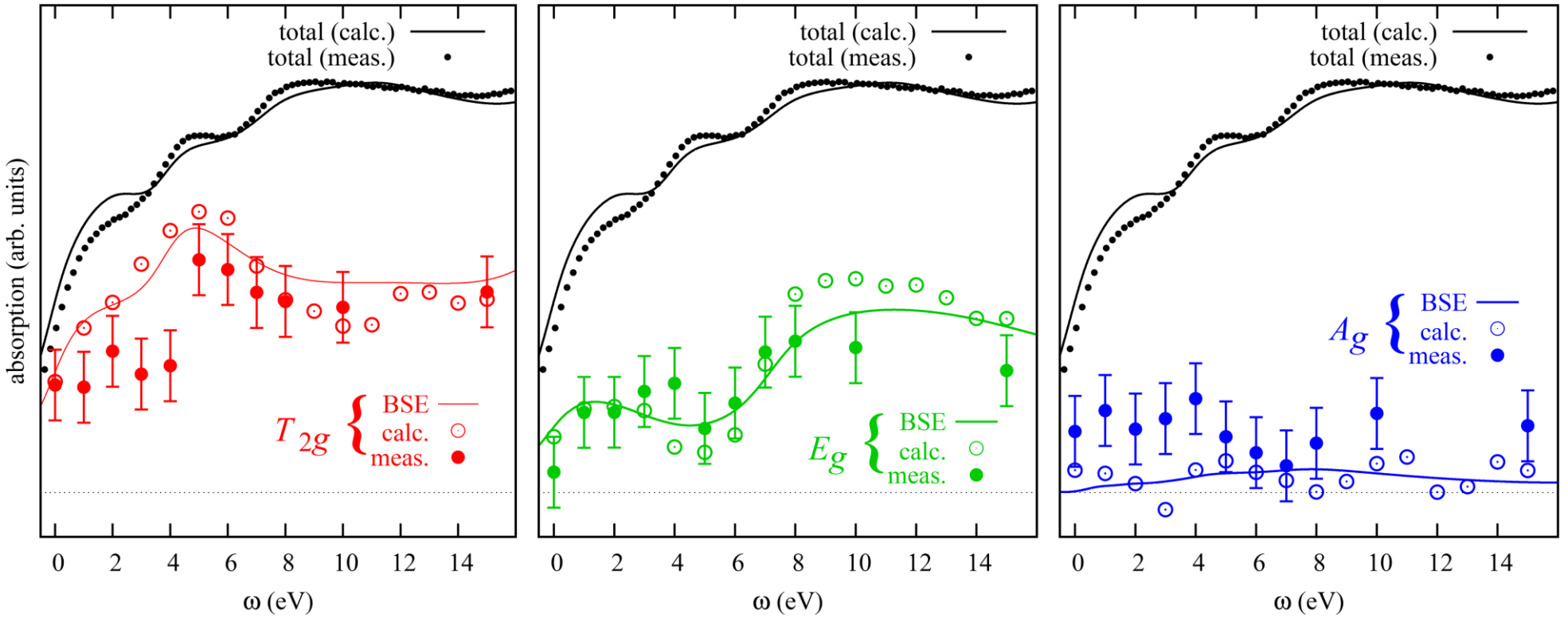

$p \rightarrow d$ (t_{2g} and e_g)
$p \rightarrow s$ (a_g)

- Complete *experimental* decomposition of L_3 *dipole* excitation …
- Achievable because of matrix elements of combined process …

Topics:

✓Ti 1*s* and Ti 2*p* photoelectron satellite structure of $SrTiO_3$ and TiO_2.

✓The “dark” $M_{4,5}$ edges of Au and Pt and the “Zeeman-Auger” effect.

- *Lattice vibrations and the d-level chemistry of CuBr.*

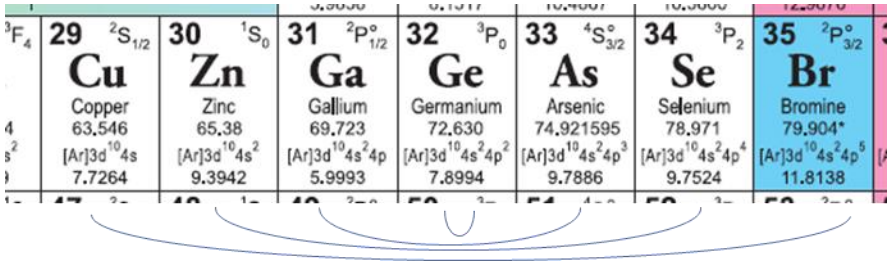

Temperature dependent NEXAFS: Ge (0)

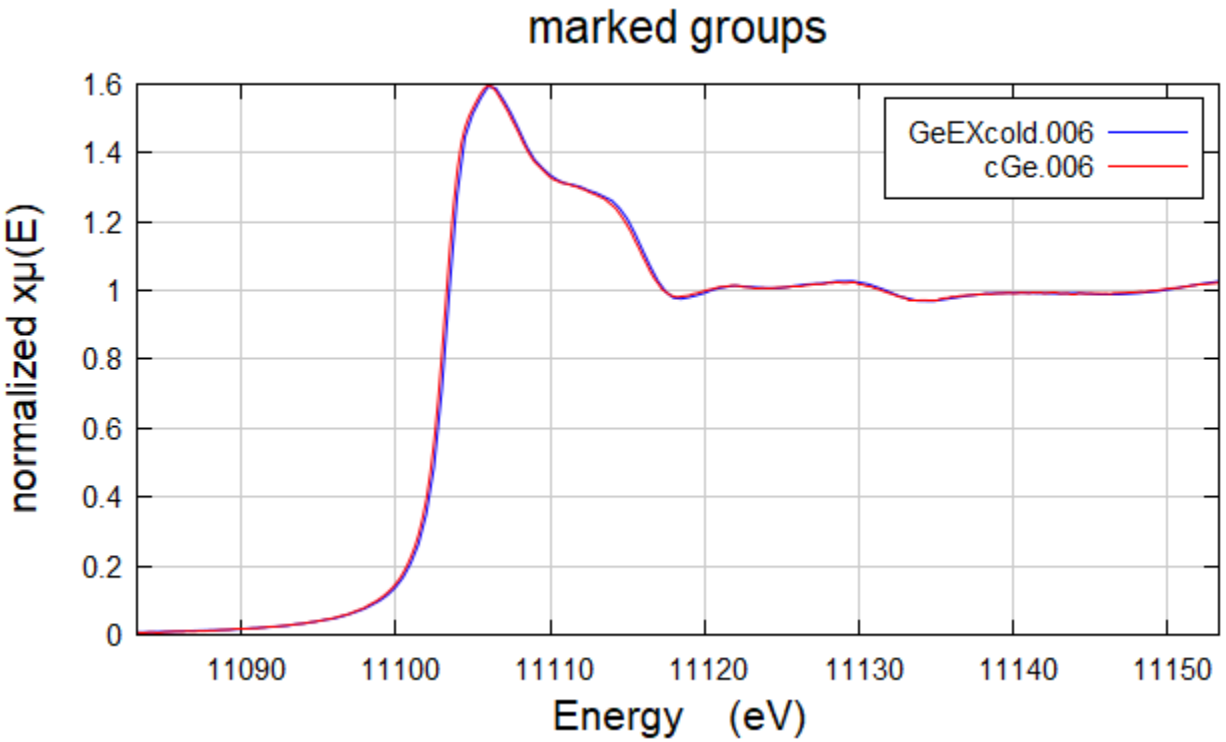

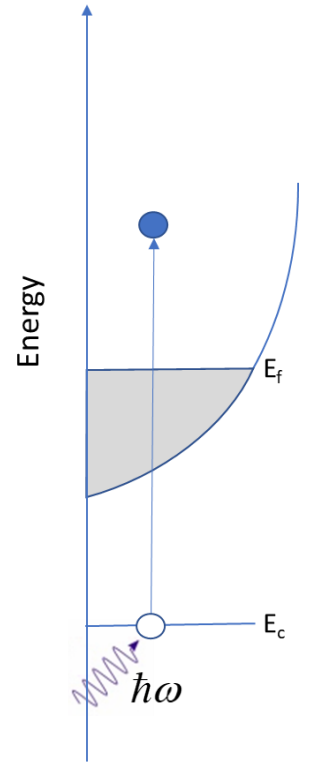

k_f ~2 Å^{-1}

EXAFS Eqn.:

$$\chi(k) = S_0^2 \sum_i N_i \left(\frac{|f_i(k)|}{kR_i^2} \right) \sin[2kR_i + \psi_i(k)]$$

$$\times \; e^{-2R_i/\lambda(k) - 2\sigma_i^2 k^2}$$

- σ^2 = Debye-Waller factor

Temperature dependent NEXAFS: GaAs (0.310)

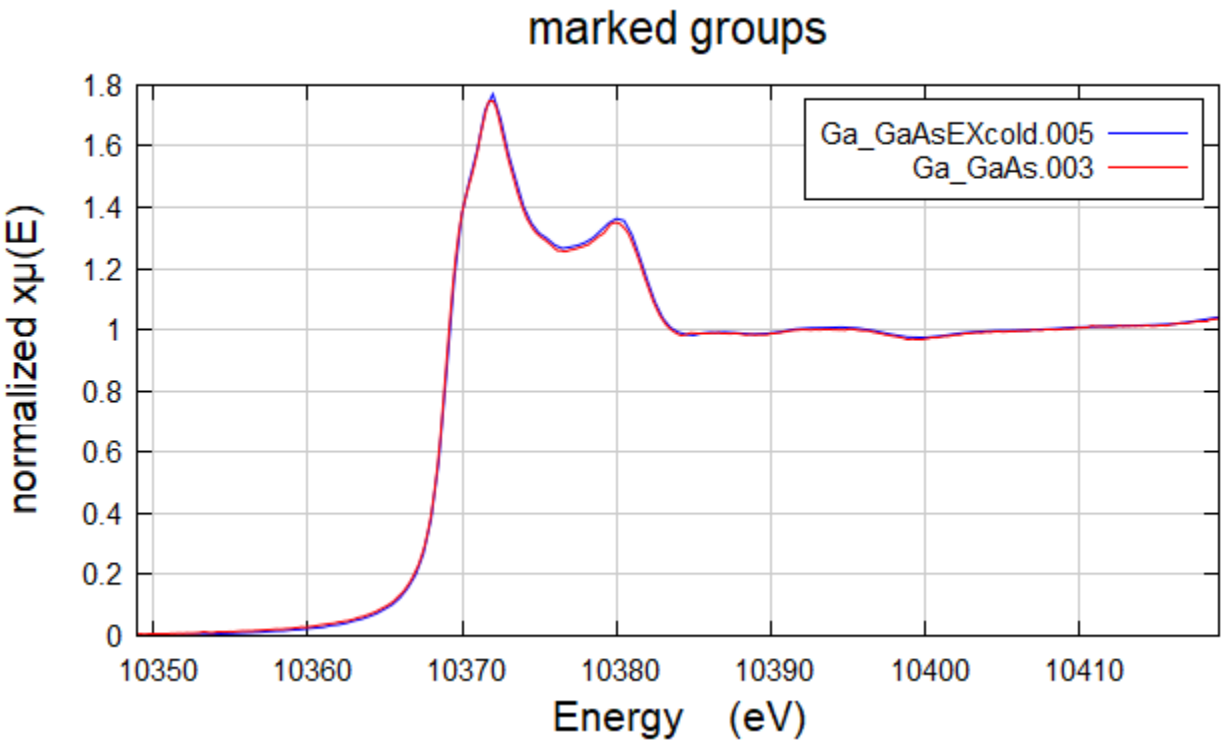

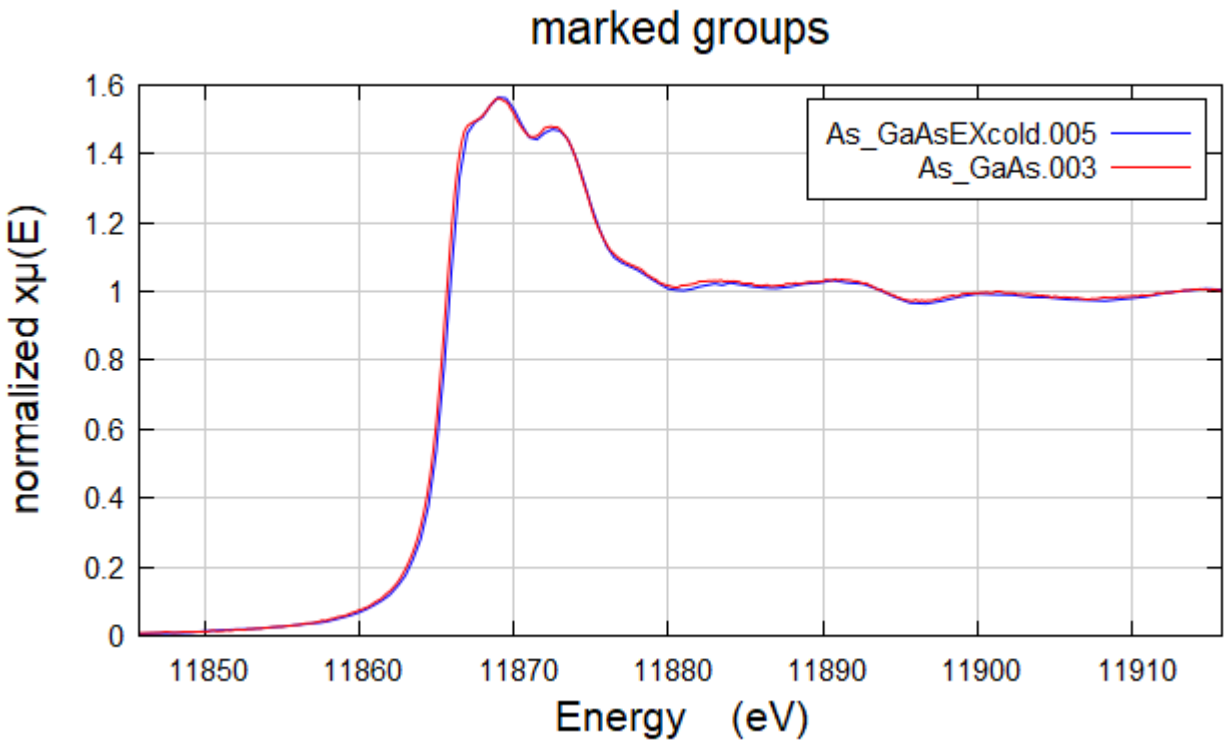

Temperature dependent NEXAFS: ZnSe (0.679)

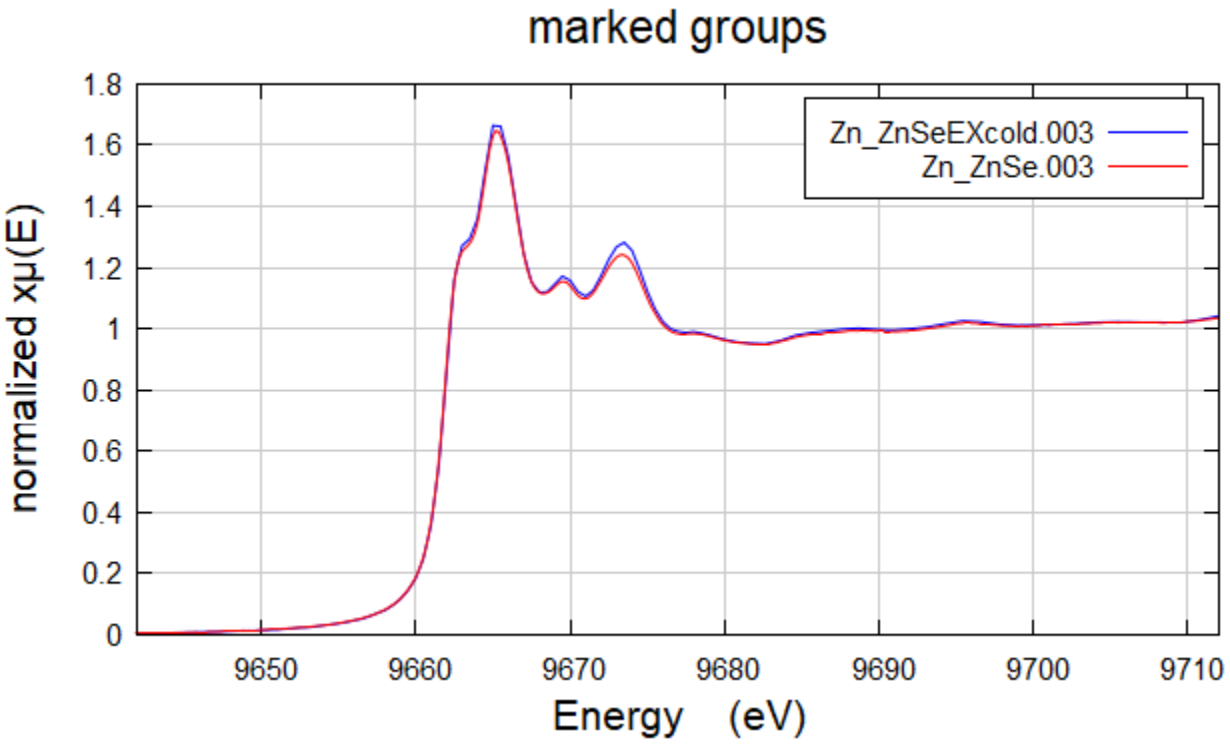

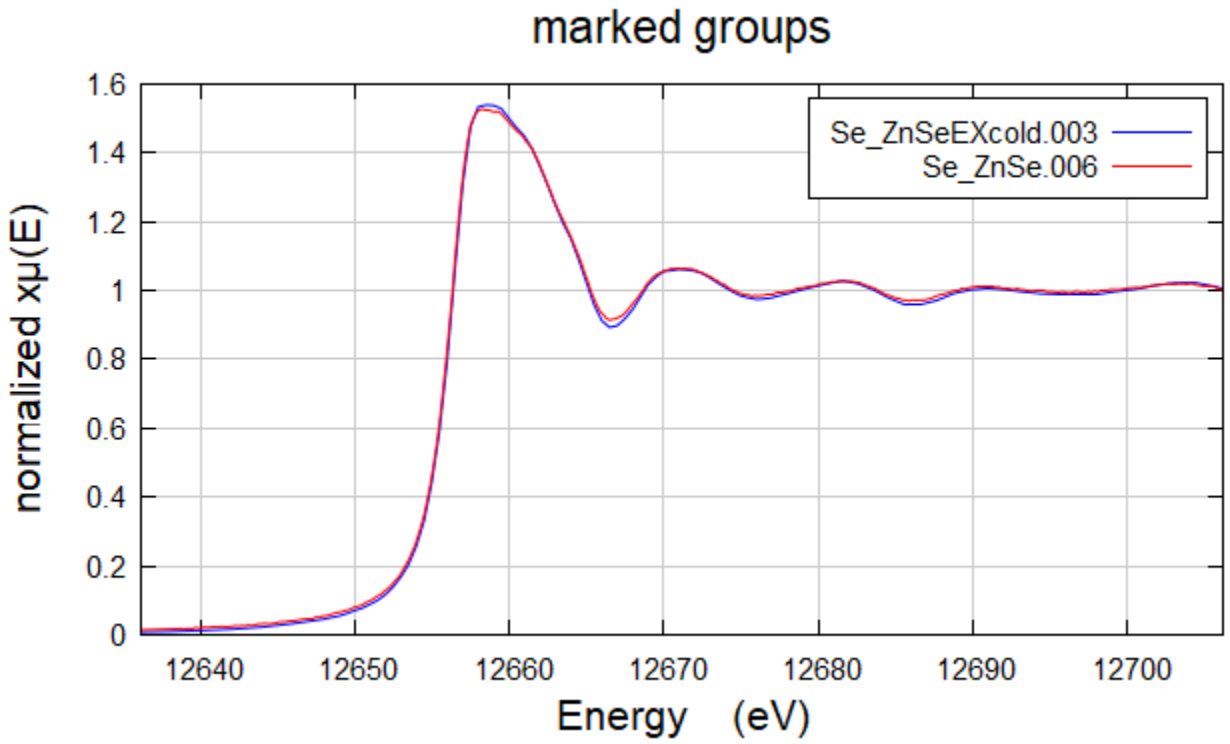

Temperature dependent NEXAFS: CuBr (0.735)

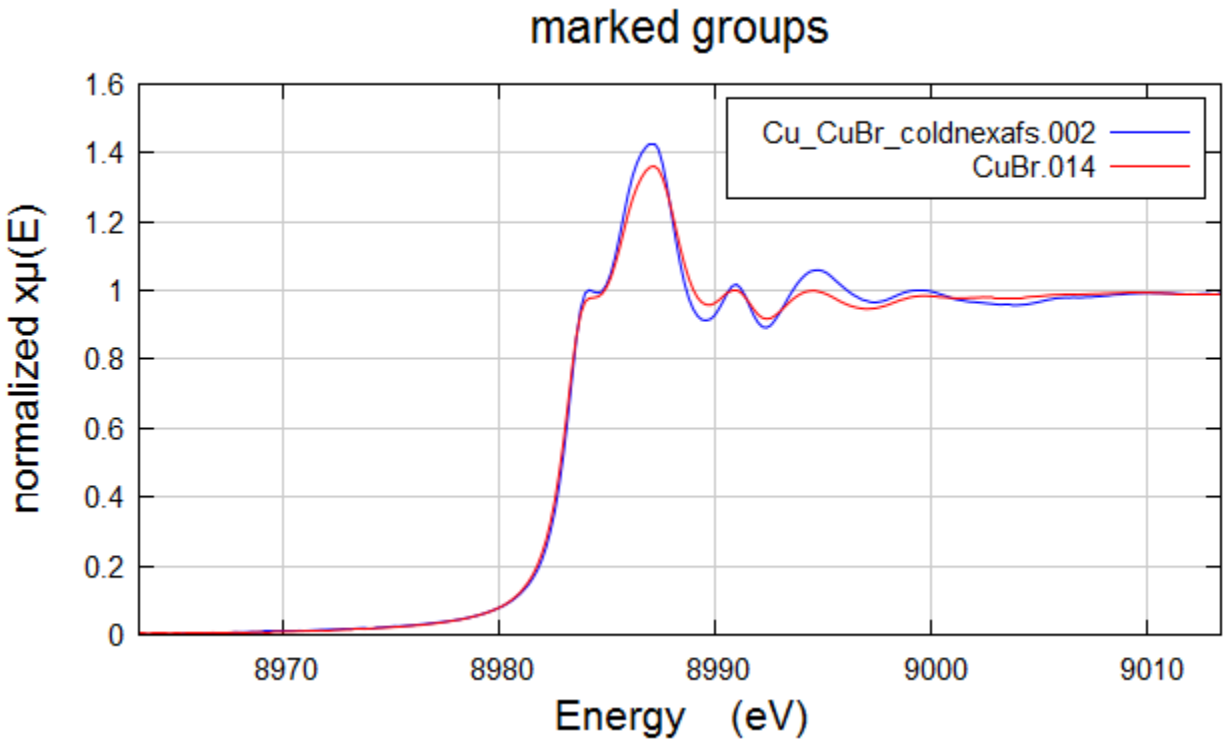

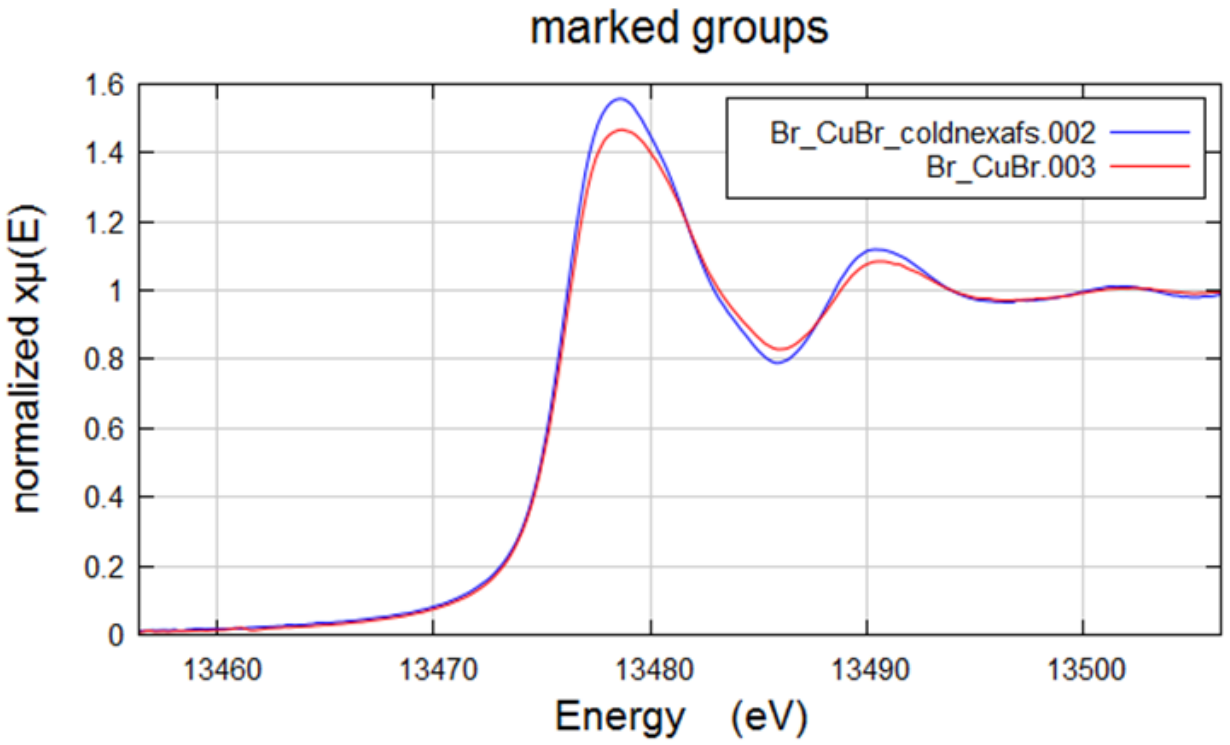

EXAFS RDF of CuBr (FT of EXAFS data: BMM)

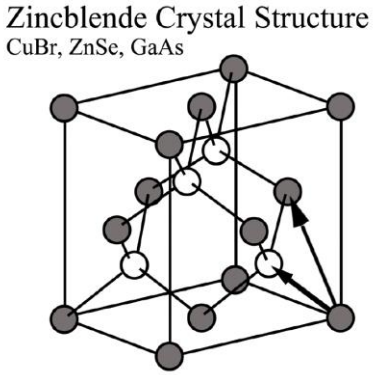

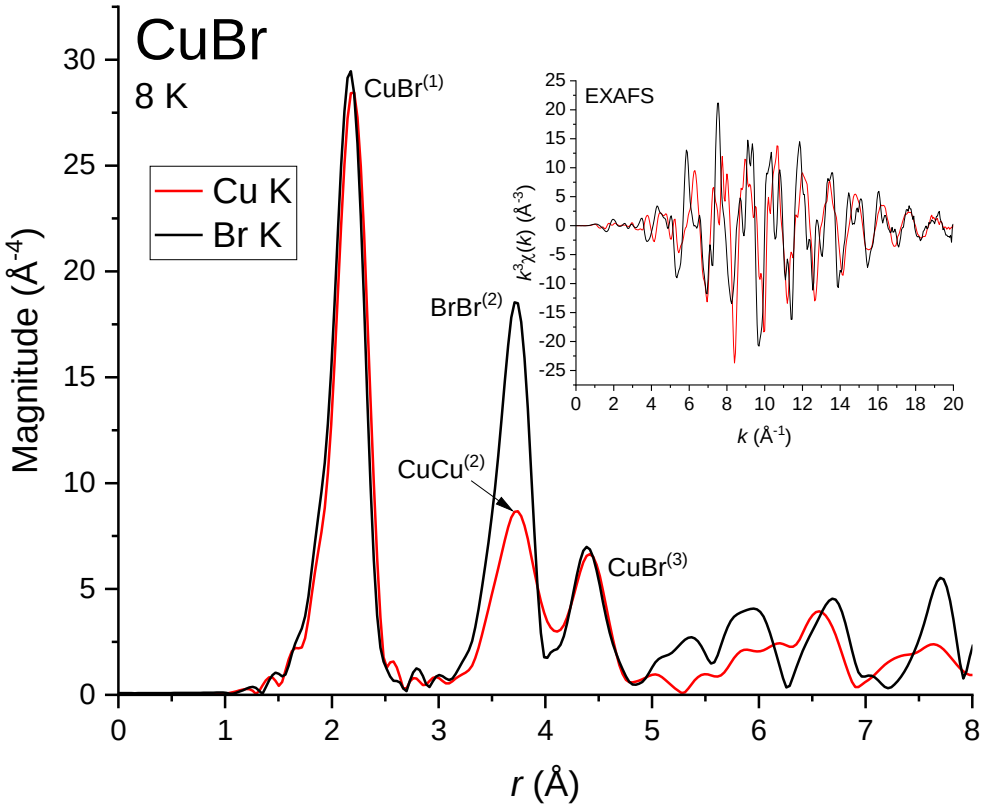

- Unlike XRD, PDF, etc., EXAFS *scattering* is chemically specific to either the Cu or Br sublattices.
- Anomalous amplitude of Cu-Cu second-neighbor distribution even at 8 K where zero-point motion dominates.

DFT Calculations of the Cu Energy Landscape

- S.-H. Wei, S.B. Zhang, and A. Zunger, *Phys. Rev. Lett.* **70**, 1639 (1993).
- C.H. Park and D.J. Chadi, *Phys. Rev. Lett.* **76**, 2314 (1996).
- S.R. Bickham *et al.*, *Phys. Rev. Lett.* **83**, 568 (1999).

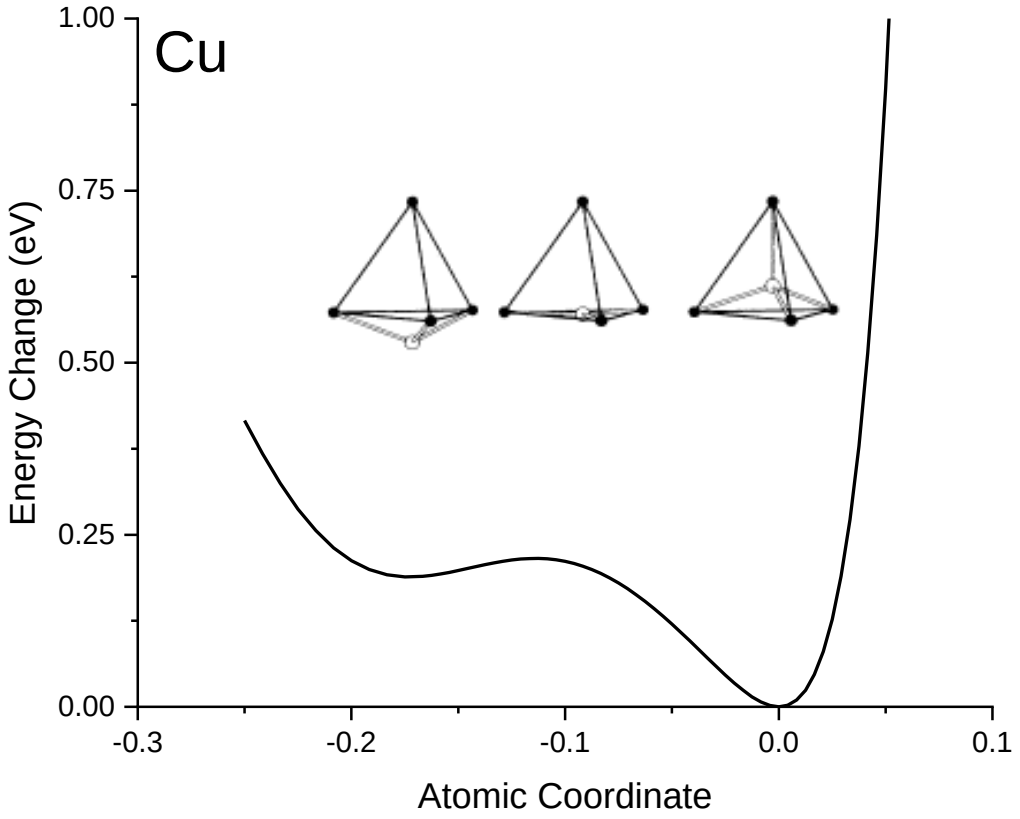

- DFT finds CuBr not stable in zincblende structure.
- *s-d vibronic* coupling.
- *Jahn-Teller* like effect.

T_d Correlation Table

T_d	T	D_{2d}	C_{3v}	C_{2v}
A_1	A	A_1	A_1	A_1
A_2	A	B_1	A_2	A_2
E	E	$A_1 + B_1$	E	$A_1 + A_2$
T_1	T	$A_2 + E$	$A_2 + E$	$A_2 + B_1 + B_2$
T_2	T	$B_2 + E$	$A_1 + E$	$A_1 + B_2 + B_1$
Other subgroups: S_4, D_2, C_3, C_2, C_s.				

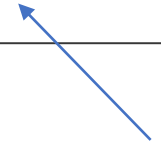

- C_{3v} symmetry splits triply degenerate T_2 set of 3*d* orbitals into doubly degenerate E set and singly degenerate A_1 set.
- A_1 set can bond with A_1 set of *s* orbitals on neighboring Cu atoms when Cu atom goes off-center.

DFT + "*U*" Calculations of the Cu Energy Landscape

- S.-H. Wei, S.B. Zhang, and A. Zunger, *Phys. Rev. Lett.* **70**, 1639 (1993).
- C.H. Park and D.J. Chadi, *Phys. Rev. Lett.* **76**, 2314 (1996).
- S.R. Bickham et al., *Phys. Rev. Lett.* **83**, 568 (1999).
- Z.-H. Wang et al., *J. Phys. Chem. Lett.* **13**, 11438 (2022).

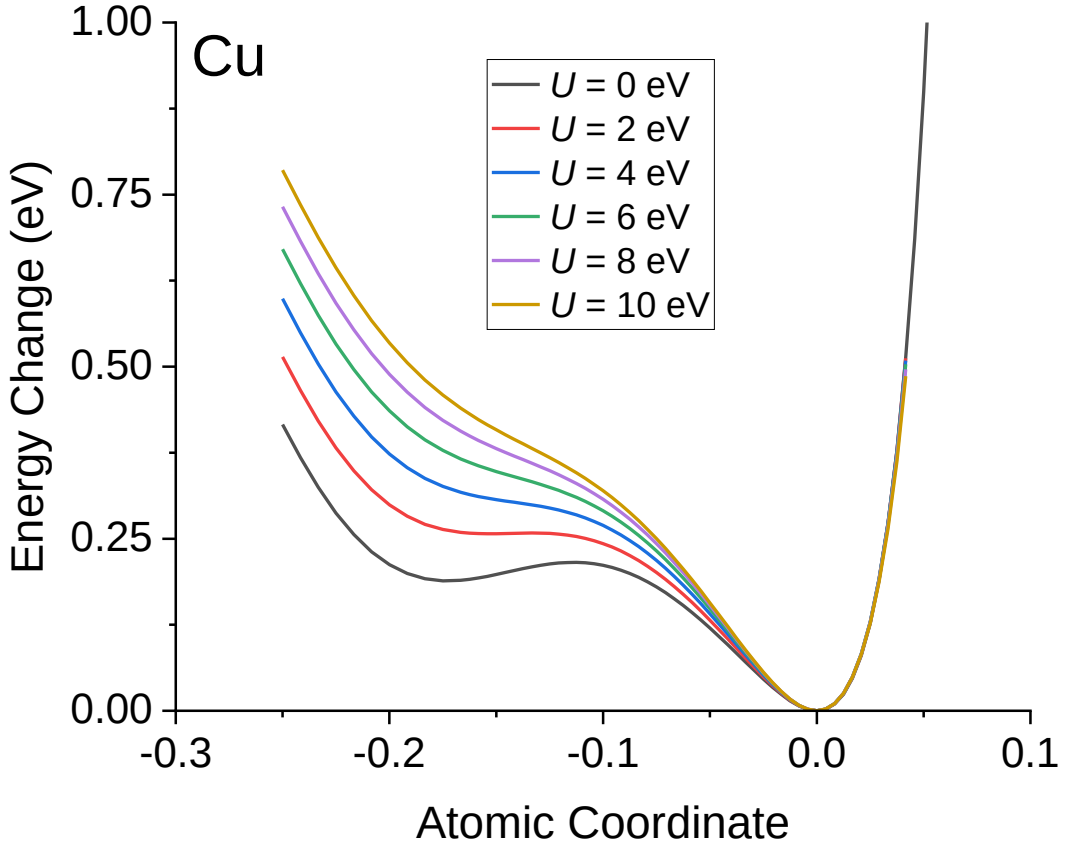

- *Hubbard* U_{Cu3d}.
- *U*: $2(3d^n) \rightarrow 3d^{n+1} + 3d^{n-1}$.
- -*U* "corrects" DFT for electron feeling its own potential (Hartree and Fock).
- CuBr stable for *U* > 2 eV!

- But, how determine *U and* what does *U* do?

Ab Initio MD Simulations of RT DW Factors

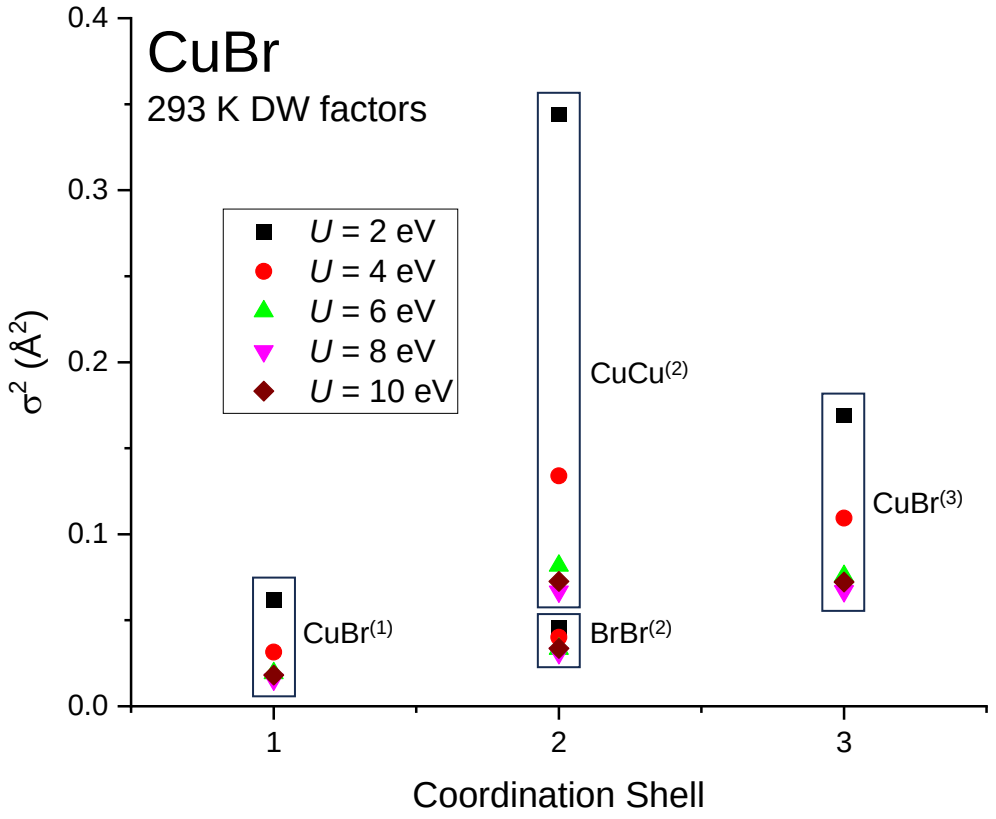

- Dramatic reduction DW factors with *U*.
- DW factors stabilize for *U* > 6 eV.
- ***Surprising*** result that *U,* which is known to localize Cu 3*d* electrons, reduces DW factors!

RT DW factors: Experiment vs. Theory *U* = 8 eV

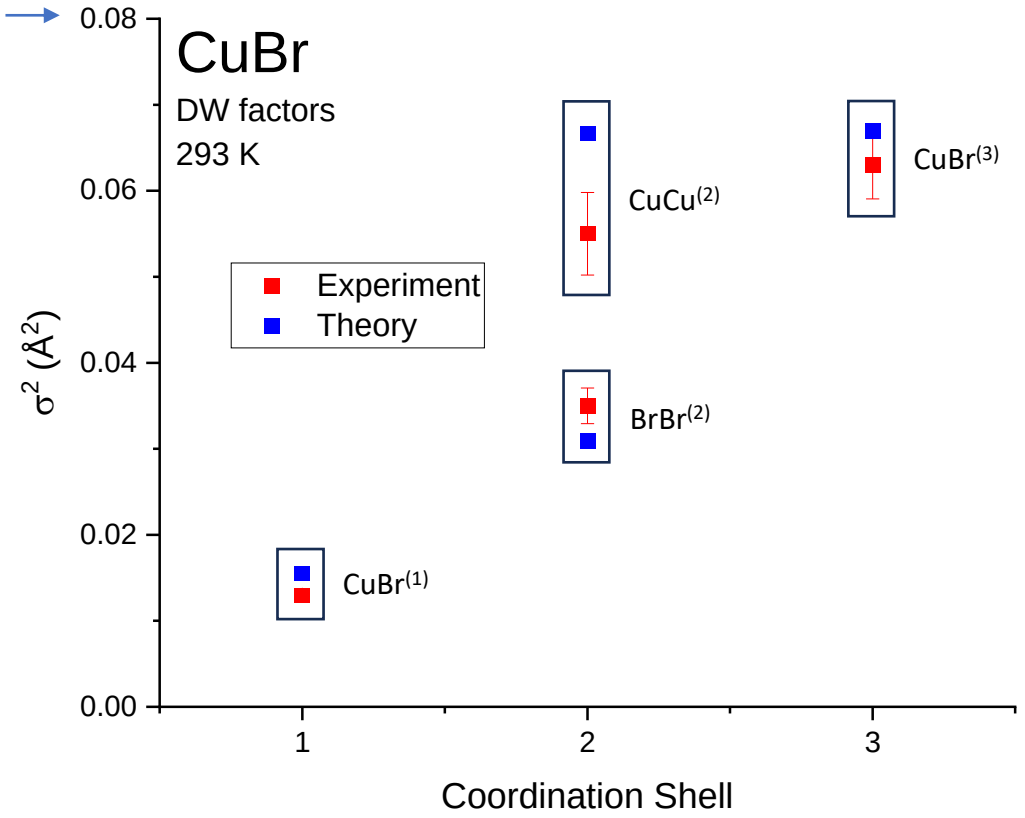

- Best agreement *U* = 8 eV …

- Note different vertical scale …

DFT Calculation of the Energy Landscape U = 8 eV

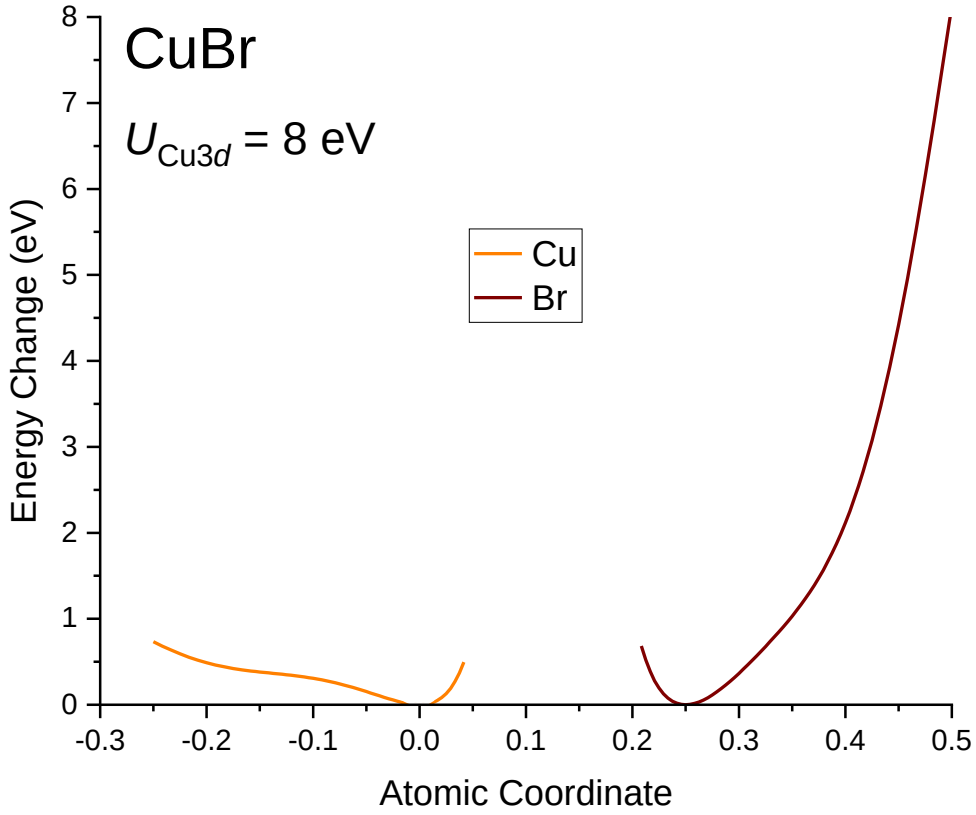

- U_{Cu3d} = 8 eV.
- Cation sublattice ¤'s >> anion sublattice ¤'s.
- Softer Cu potential-energy curve.
- "Hard-sphere" limit encountered for each as they move toward each other.

Energy Landscape CuBr, ZnSe, GaAs, and Ge

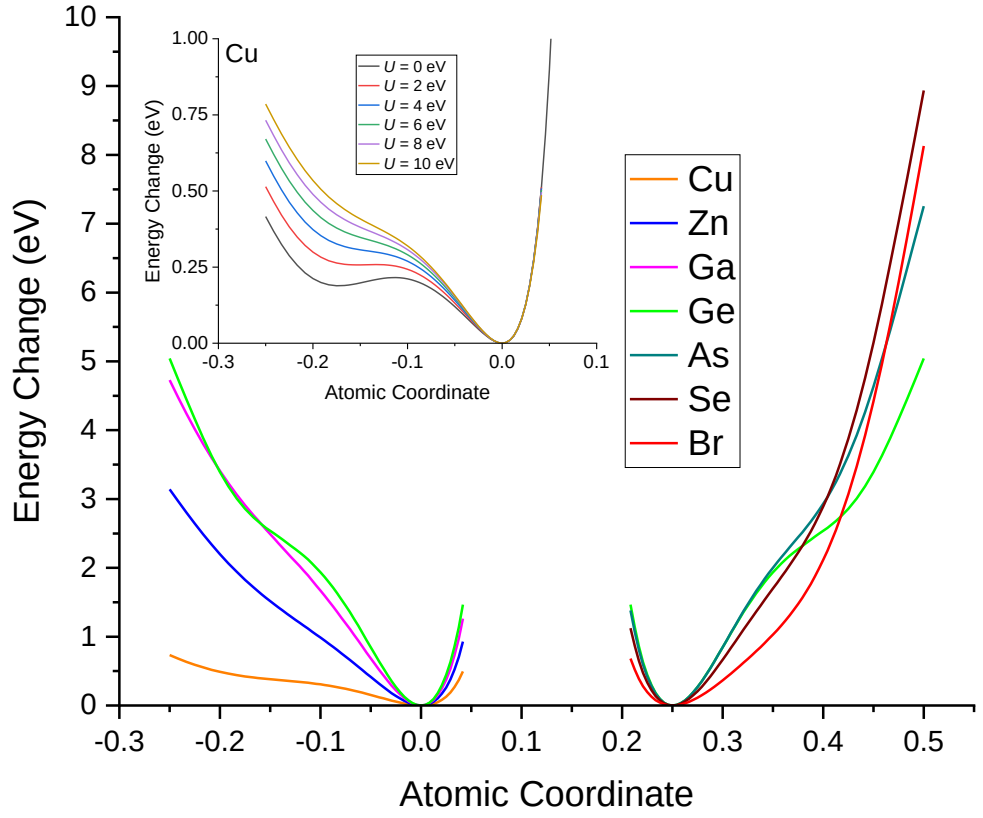

- U_{Cu3d} = 8 eV.
- Cation sublattice ¤'s >> anion sublattice ¤'s.
- Softer cation potential-energy curve.
- "Hard-sphere" limit encountered for each as they move toward each other.
- *s-d* coupling intrinsic for all cations, but it becomes less important as *d*-level binding energy increases with *Z*.

Experimental (EXAFS) and theoretical (MD-DFT) Debye-Waller factors

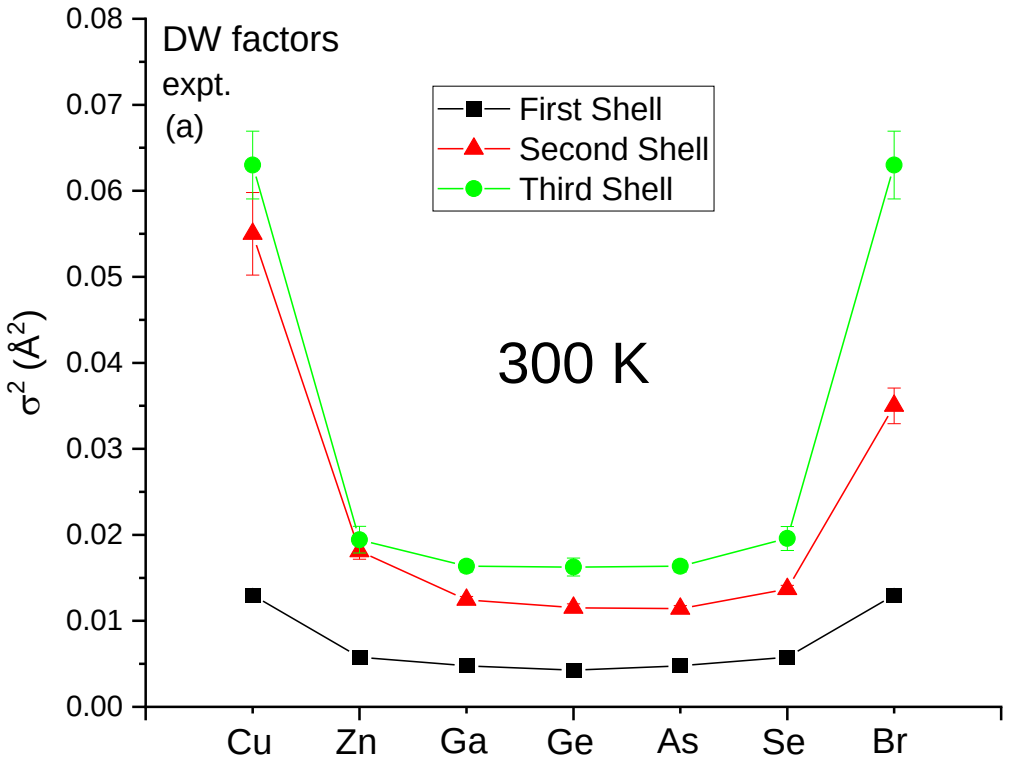

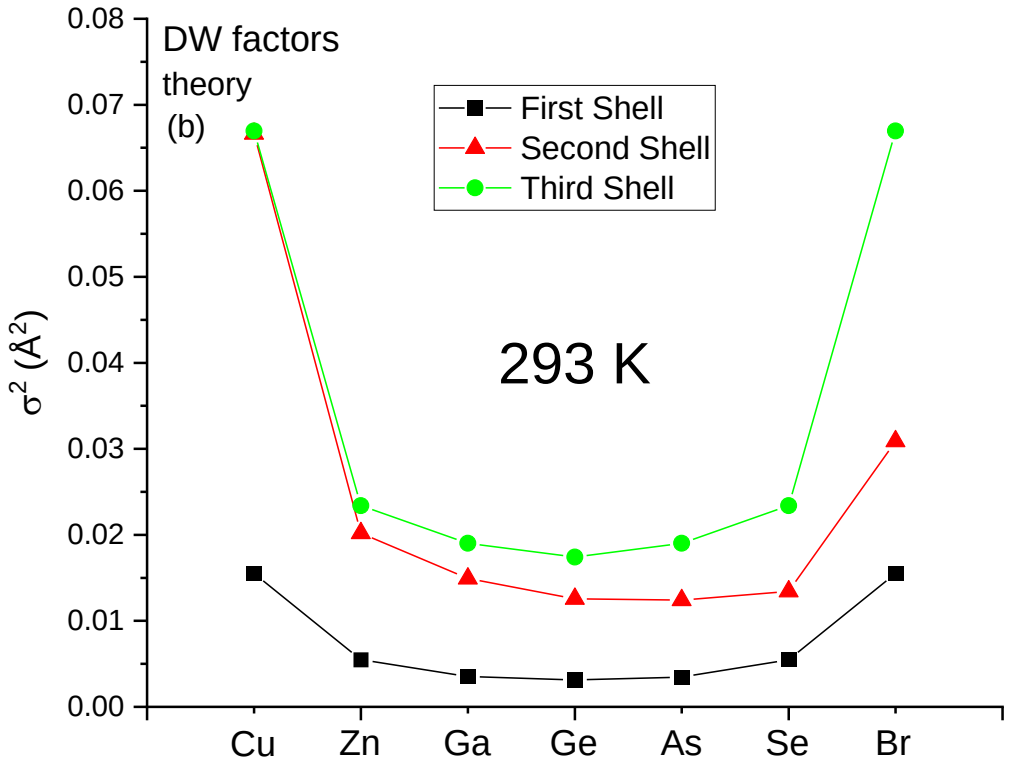

- Vibrations are an increasing function of ionicity.
- Cation vibrations are always larger than anion vibrations.
- Direct reflection of stronger covalent versus ionic bonding.

Cu K-edge NEXAFS

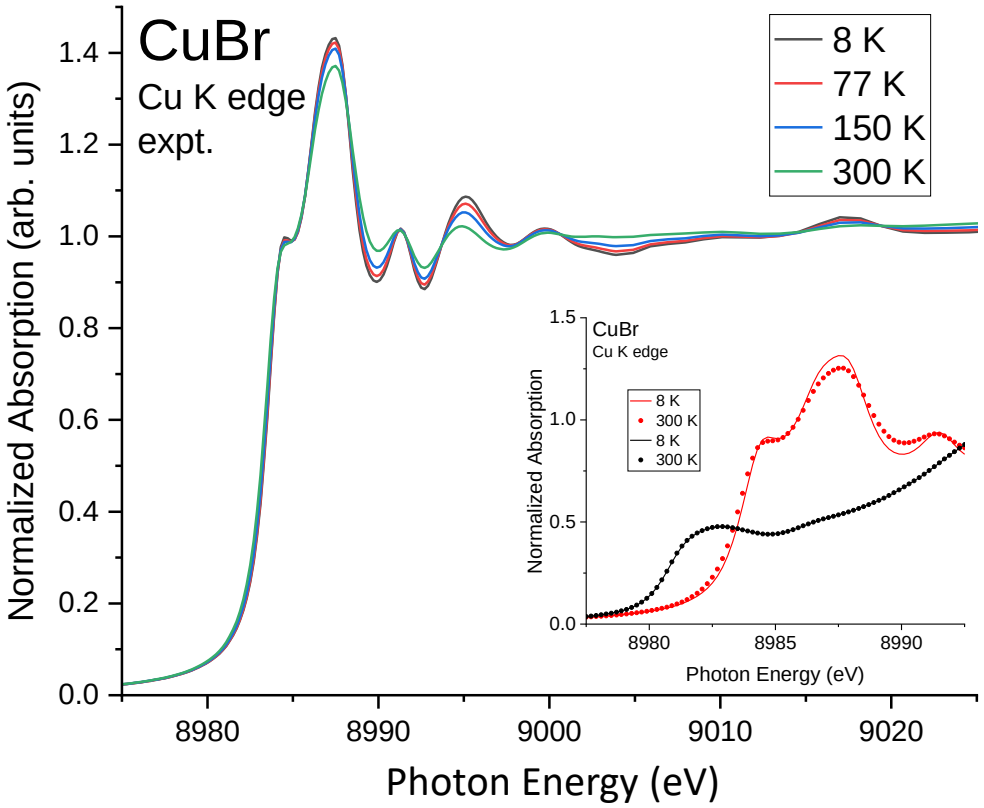

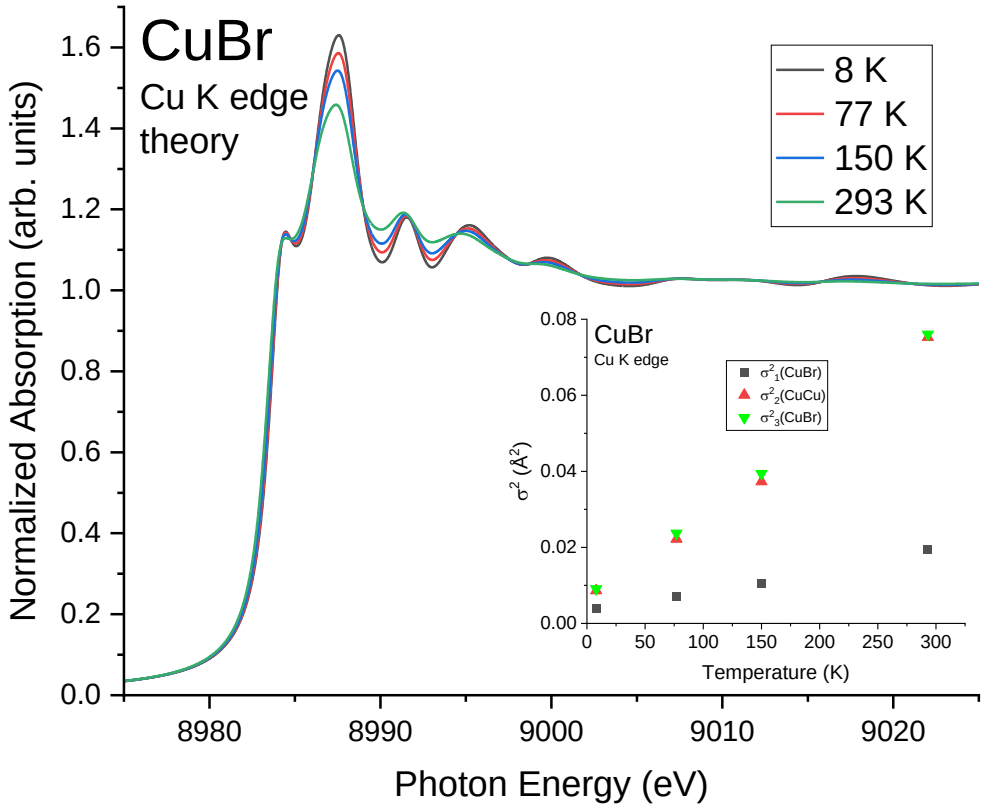

Br K-edge NEXAFS

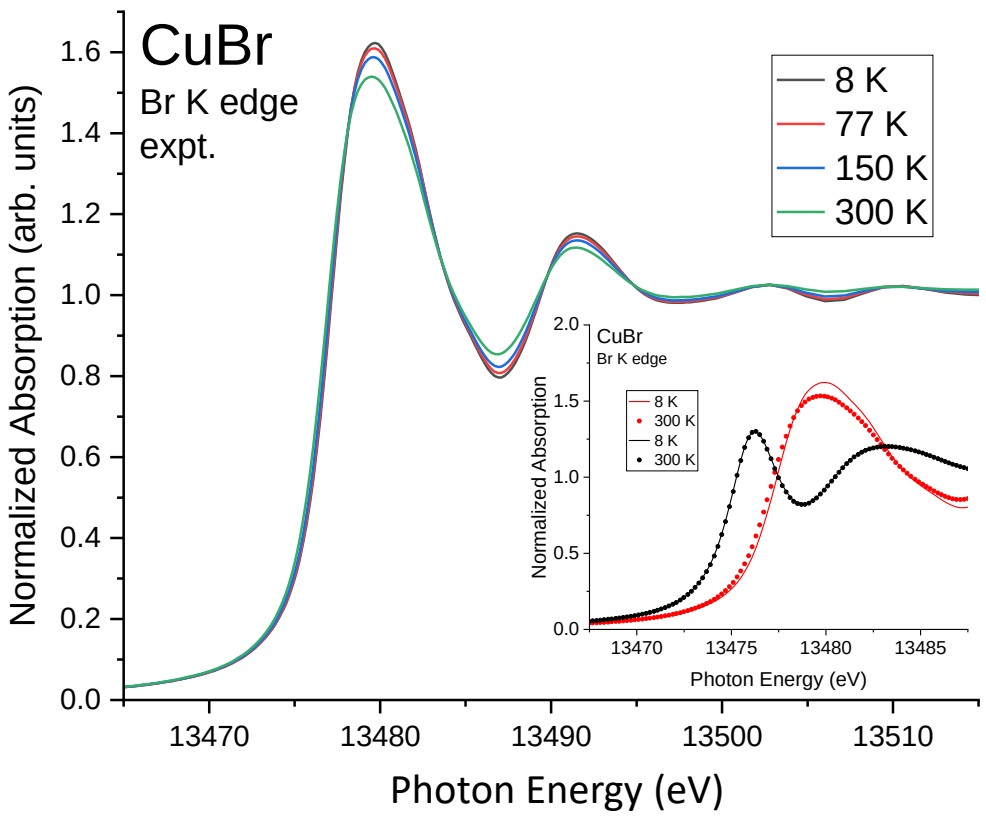

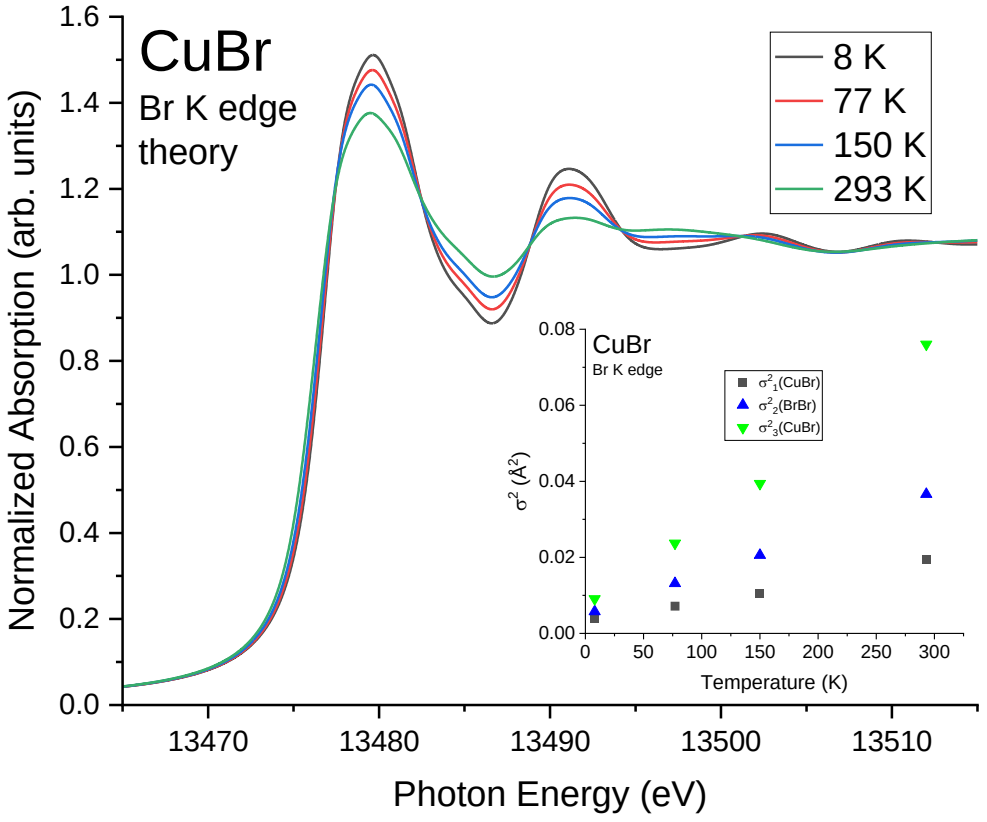

Electronic Structure and Chemical Bonding of CuBr: What does "U" do?

Cu [Ar] $3d^{10}\,4s^{1}$ → e^- → Cu^+ [Ar] $3d^{10}$

Br [Ar] $3d^{10}\,4s^{2}\,4p^{5}$ → e^- → Br^- [Ar] $3d^{10}\,4s^{2}\,4p^{6}$

Ge [Ar] $3d^{10}\,4s^{2}\,4p^{2}$

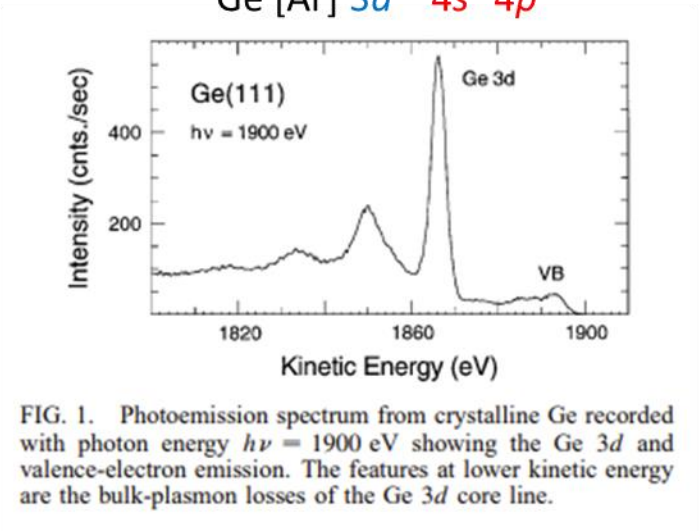

FIG. 1. Photoemission spectrum from crystalline Ge recorded with photon energy $h\nu = 1900$ eV showing the Ge $3d$ and valence-electron emission. The features at lower kinetic energy are the bulk-plasmon losses of the Ge $3d$ core line.

- Noble-gas *like* outer shells …

Binding Energy (eV)

Cu $3d$ 1.5, 1.8
Cu $4s$ 1.2

Br $3d$ 69.0, 70.1
Br $4s$ 27.3
Br $4p$ 4.6, 5.2

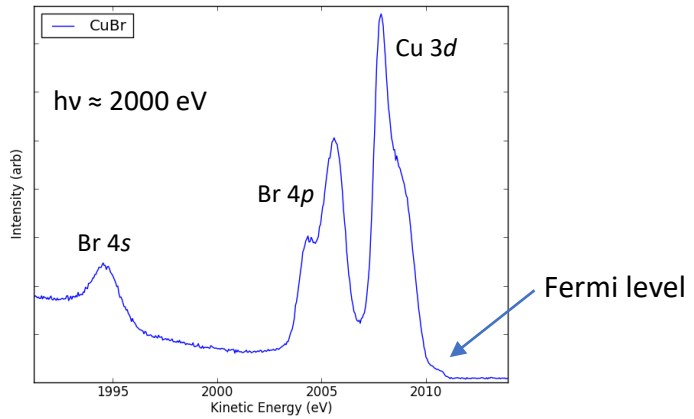

J.C. Woicik, E.J. Nelson, and P. Pianetta, *Phys. Rev. Lett.* **84**, 773 (2000).

Molecular Orbital Diagram T_d Symmetry

- A. Goldmann, J. Tejeda, N.J. Shevchik, and M. Cardona, *Phys. Rev. B* **10**, 4388 (1994).

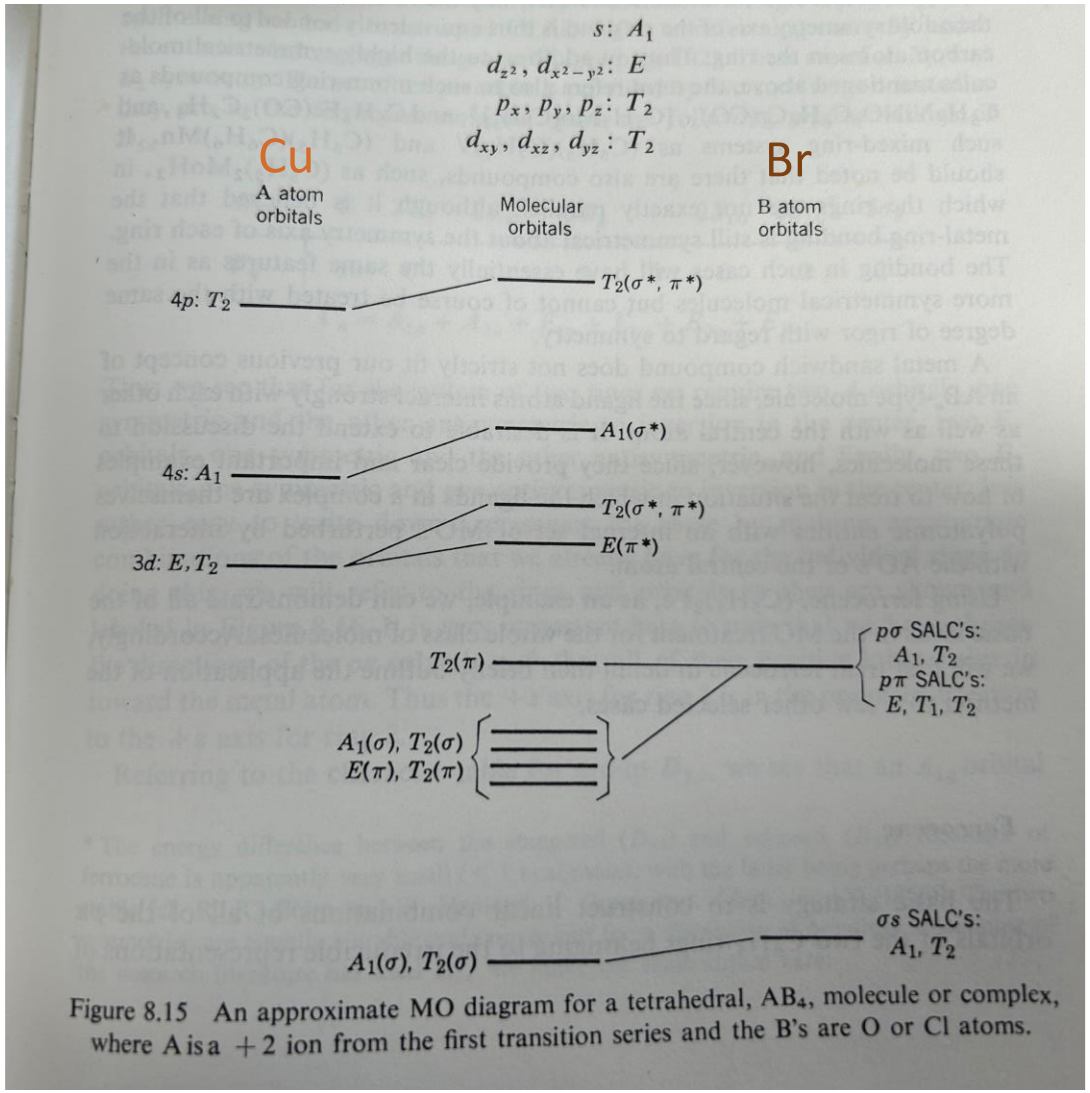

Figure 8.15 An approximate MO diagram for a tetrahedral, AB_4, molecule or complex, where A is a +2 ion from the first transition series and the B's are O or Cl atoms.

- Note Br 4*p* bonding and Cu 3*d* anti-bonding states fully occupied …
- Presence of gap in occupied states …
- Warrants a further look …

F.A. Cotton, *Chemical Applications of Group Theory,* Wiley (1971).

Photoemission Valence Band CuBr

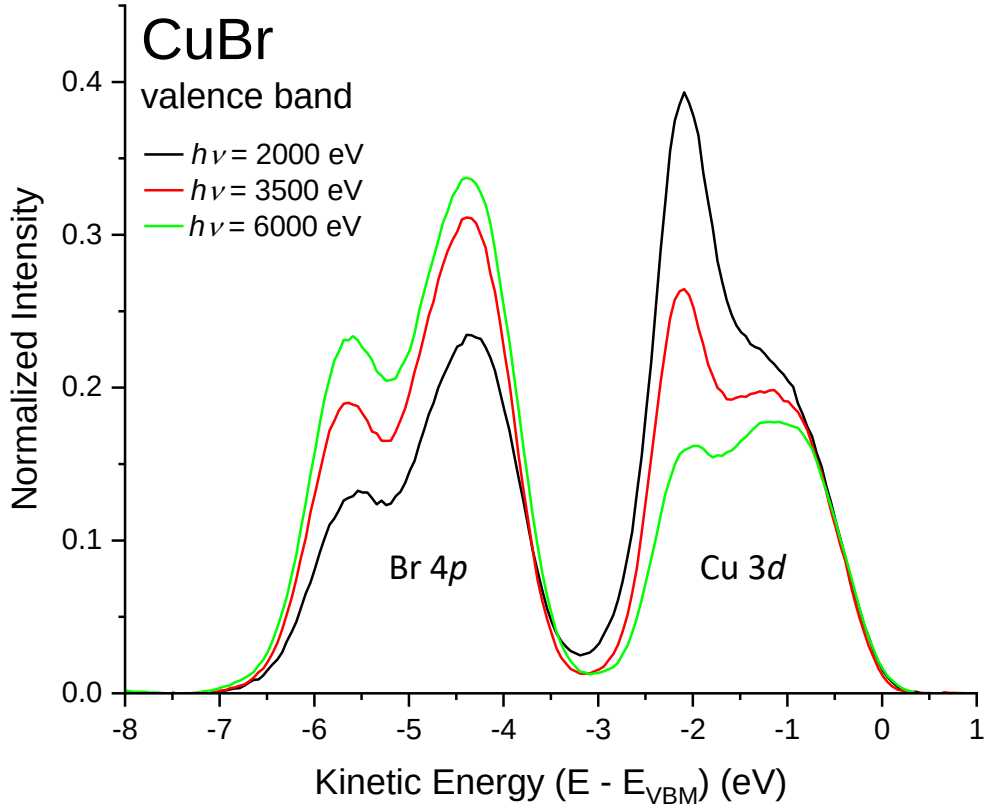

$\frac{\sigma(\text{Cu } 3d)}{\sigma(\text{Br } 4p)}$ @ 2000 eV = 1.23

$\frac{\sigma(\text{Cu } 3d)}{\sigma(\text{Br } 4p)}$ @ 6000 eV = 0.31

- Note *both* intensity *and* shape variation of bands …

Hybridization and Bond-Orbital Components in Site-Specific X-Ray Photoelectron Spectra of Rutile TiO_2

J. C. Woicik,[1] E. J. Nelson,[1] Leeor Kronik,[2] Manish Jain,[2] James R. Chelikowsky,[2] D. Heskett,[3] L. E. Berman,[4] and G. S. Herman[5]

Phys. Rev. Lett. **89**, 077401 (2002).

$$I(E, h\nu) \propto \sum_{i,l} \rho_{i,l}(E)\sigma_{i,l}(E, h\nu). \qquad (1)$$

Here E is the photoelectron binding energy, $h\nu$ is the x-ray photon energy, $\rho_{i,l}(E)$ are individual, angular-momentum l resolved, electronic single-particle partial density of states of the ith atom of the crystalline-unit cell, and $\sigma_{i,l}(E, h\nu)$ are the angle-integrated, angular-momentum dependent, photoionization cross sections.

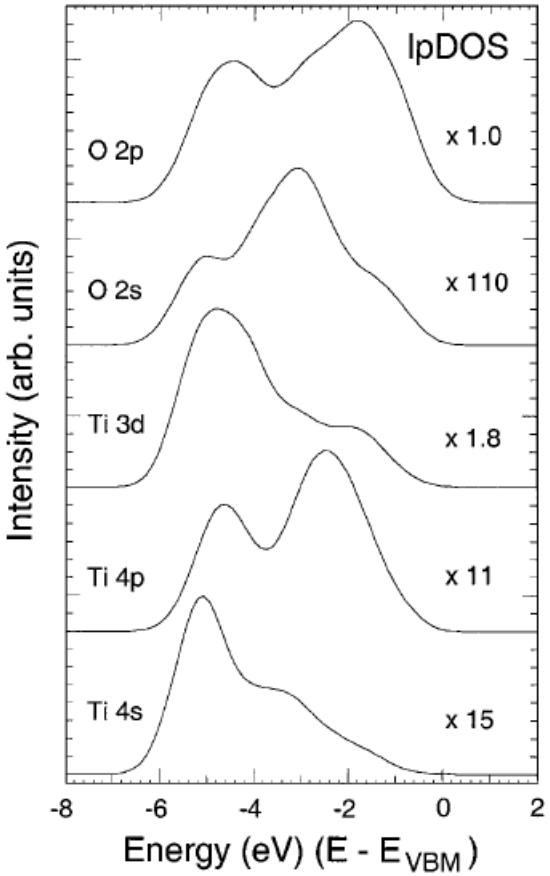

FIG. 4. The different *angular-momentum* components of the theoretical Ti and O partial density of states. Multipliers relative to the O $2p$ component are indicated in each case.

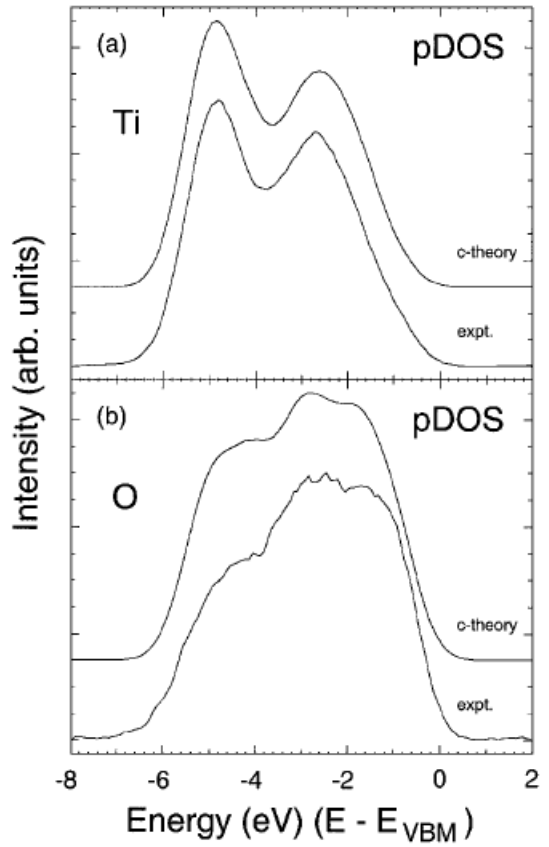

FIG. 5. Theoretical partial density of states corrected for individual angular-momentum dependent photoelectron cross sections and the site-specific experimental valence-photoelectron spectrum: (a) Ti; (b) O. The curves have been scaled to equal peak height.

Principal Component Analysis (PCA) of VB

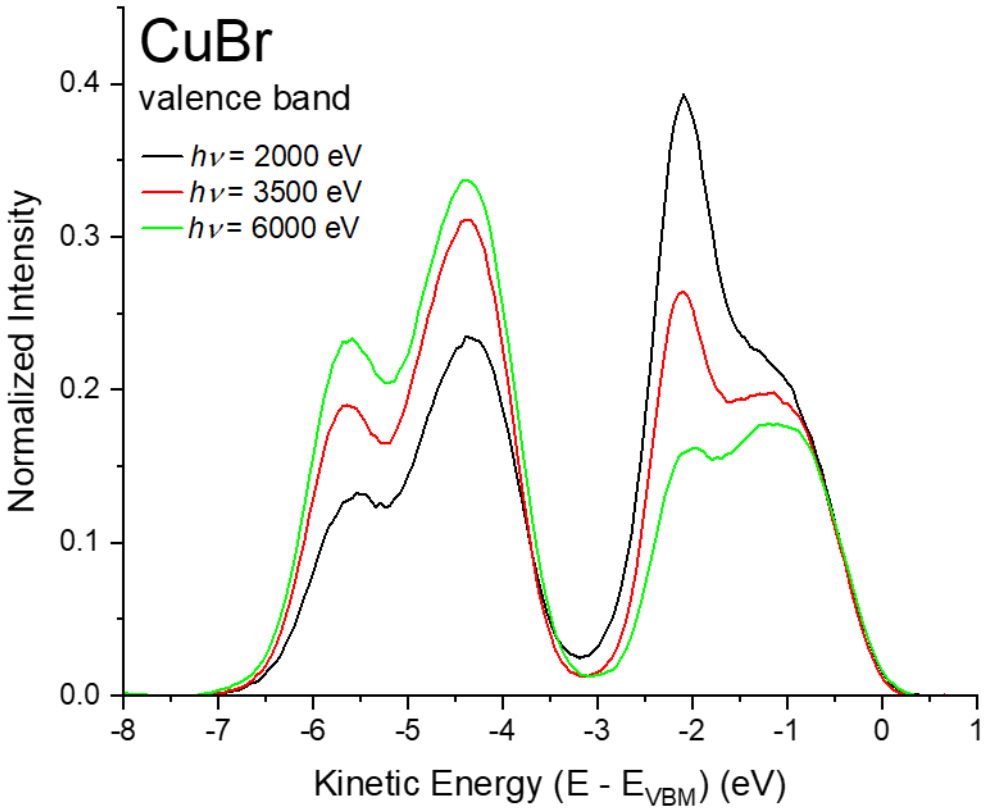

- Note "strength" of σ versus π bonding …

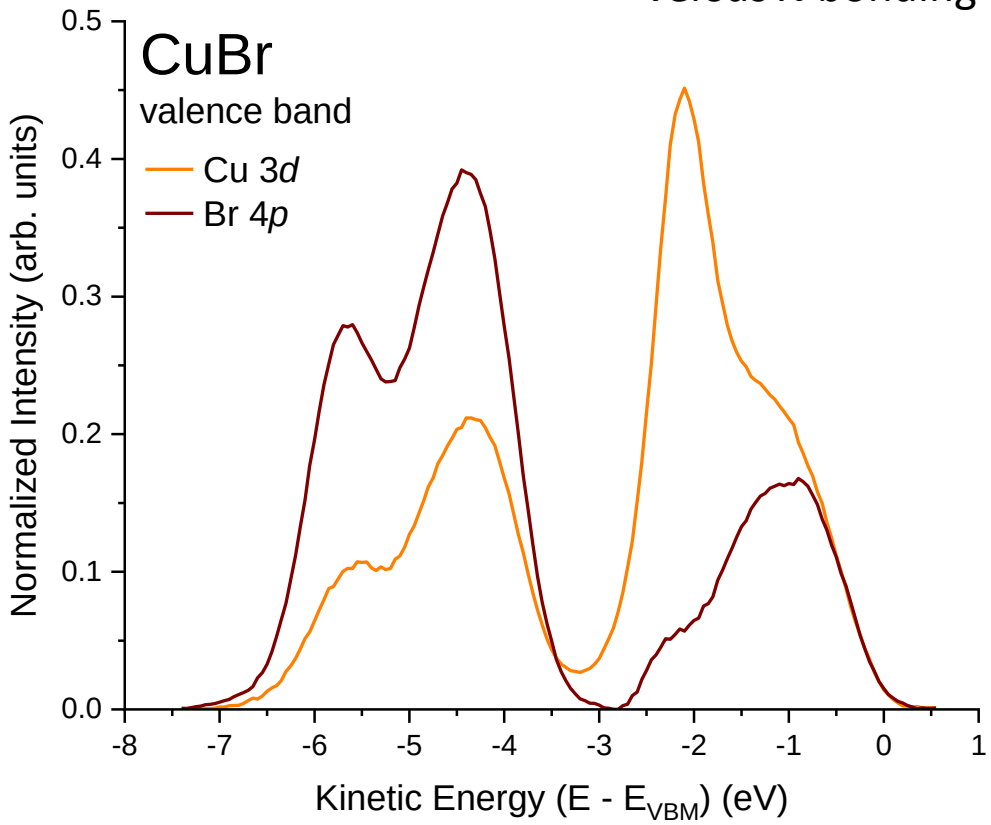

- Direct *experimental observation* of the sharing of electrons in a covalent bond ...

DFT Density of States

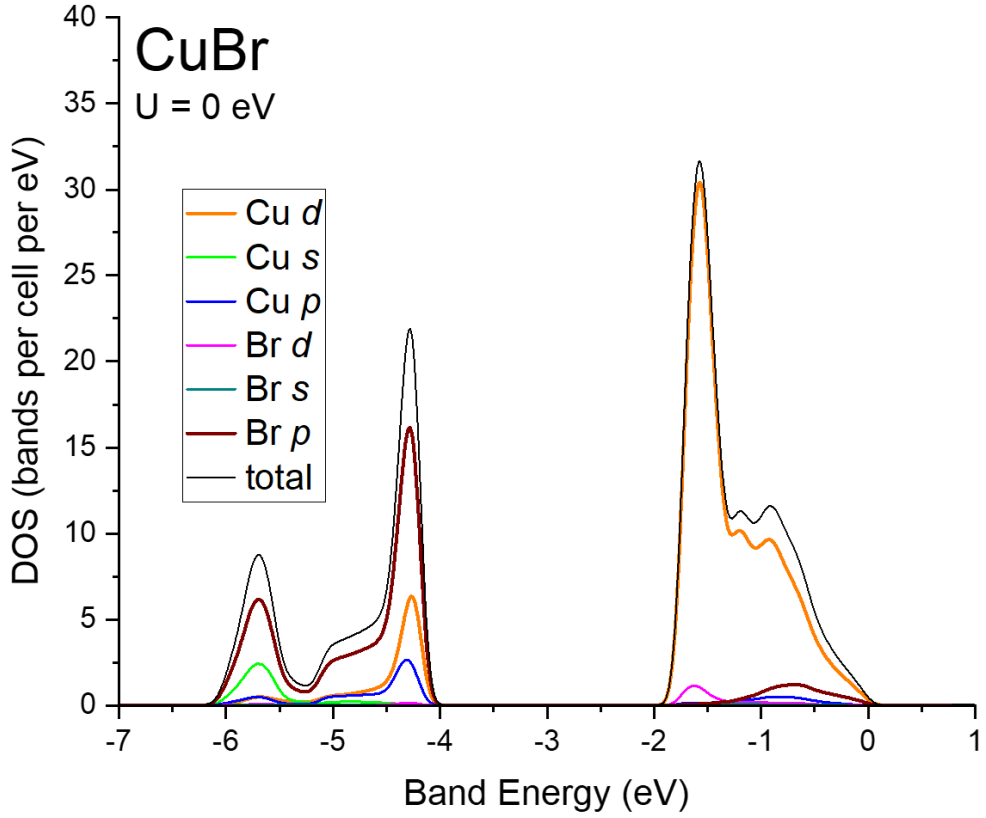

DFT + "*U*" Density of States

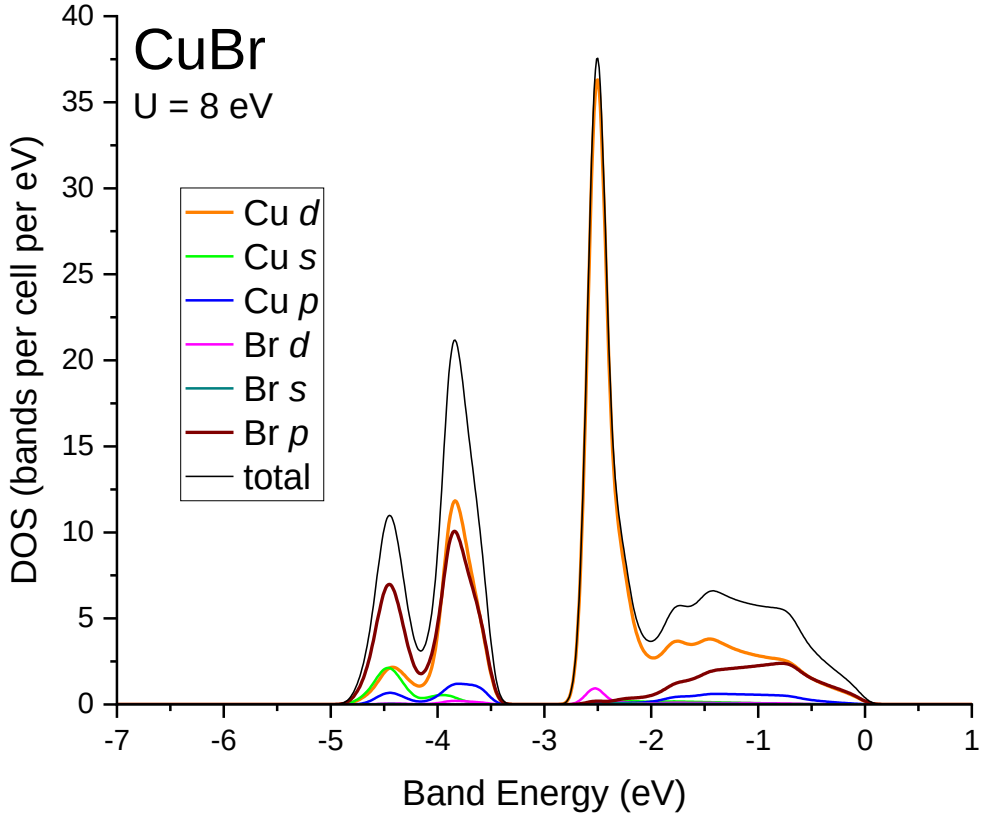

- *U* lowers energy of Cu 3*d* states therefore increases overlap and hence chemical bonding with Br 4*p* states.
- Covalency and increased strength of Cu-Br bond directly observed by photoemission and reduction of DW factors!
- Stronger Cu-Br bond overcomes anomalously strong *s*-*d* coupling in DFT …

Why BSE/DFT-LDA work?

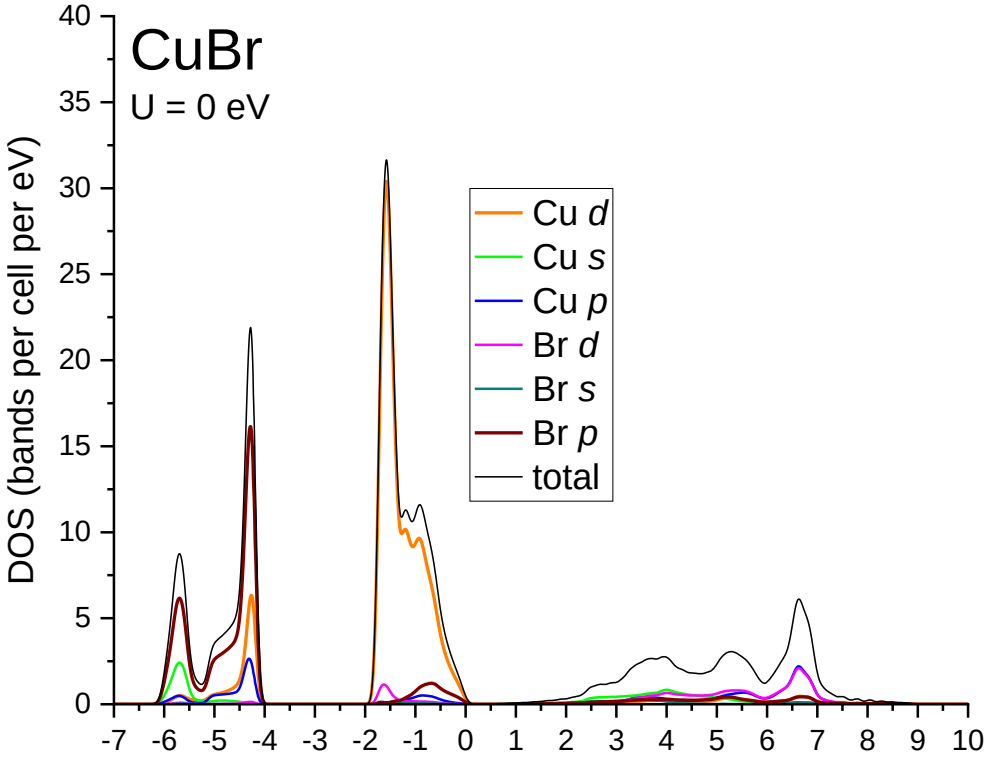

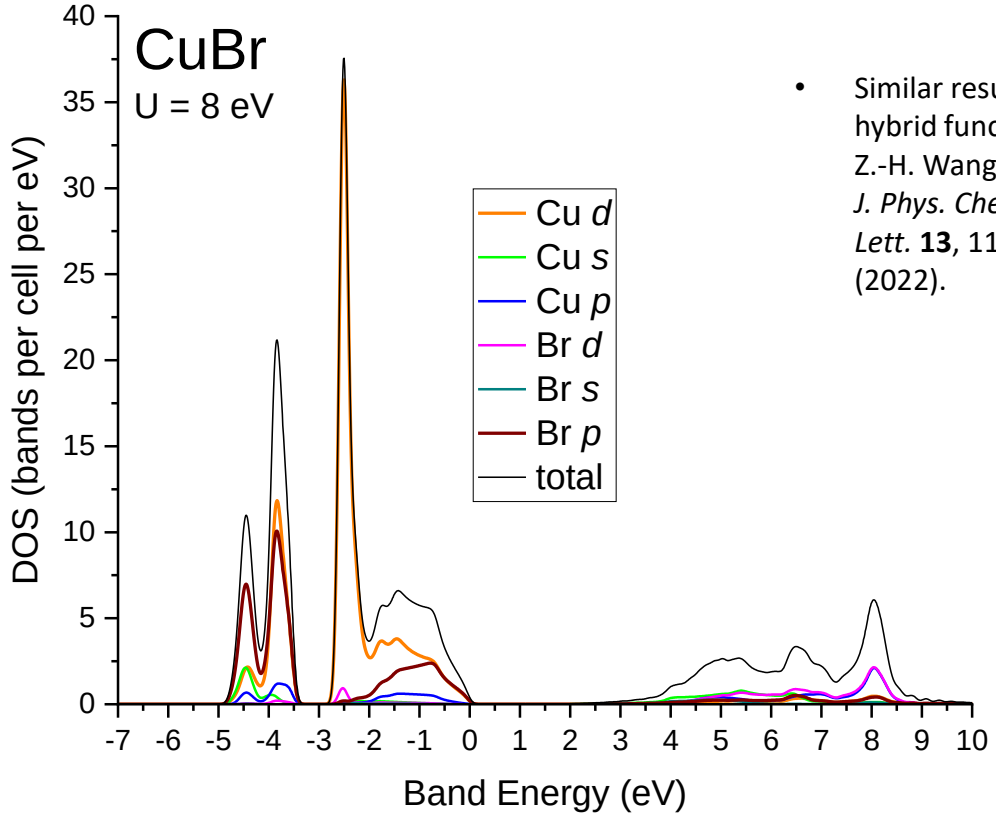

- Similar result as hybrid functional: Z.-H. Wang *et al.*, *J. Phys. Chem. Lett.* **13**, 11438 (2022).

- *U* little effect on unoccupied DOS (XAFS)…
- Increase of bandgap with *U* also limits effect of *s-d* vibronic coupling …

Additional Topics

On the nature of S_0^2 and a quote from Ed.

- AND –

The need for LRO theory of NEXAFS.

S 1*s* photoemission MoS_2

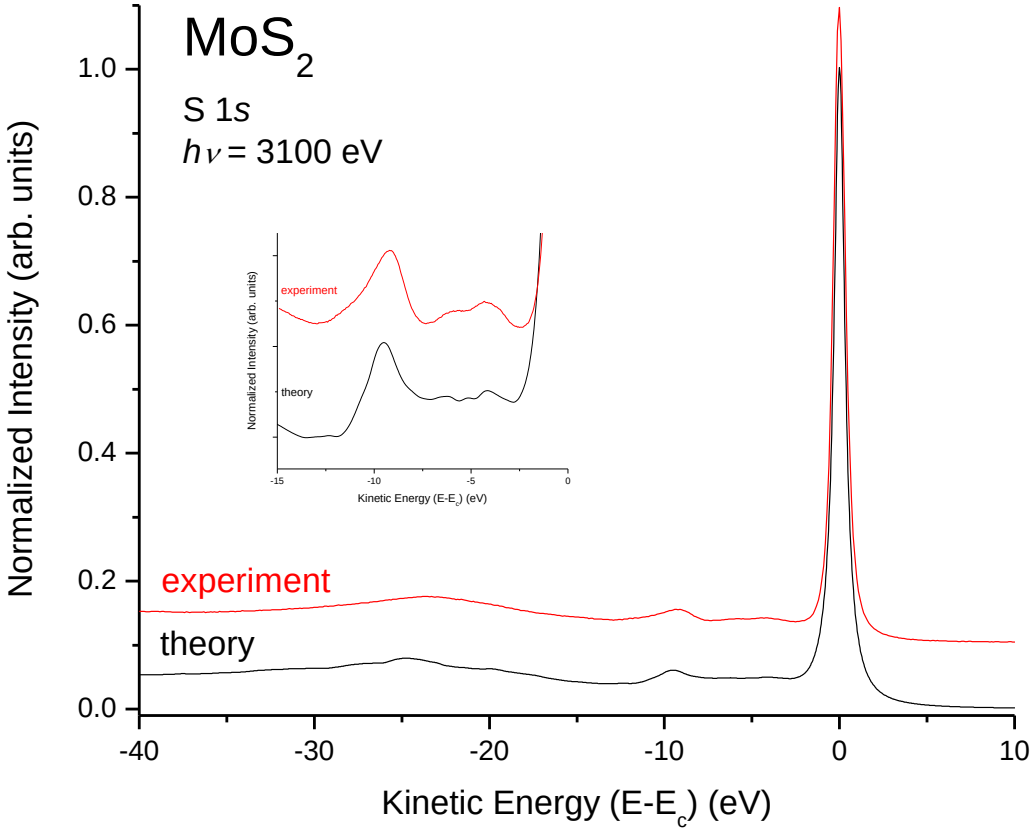

S *KLL* Auger MoS_2

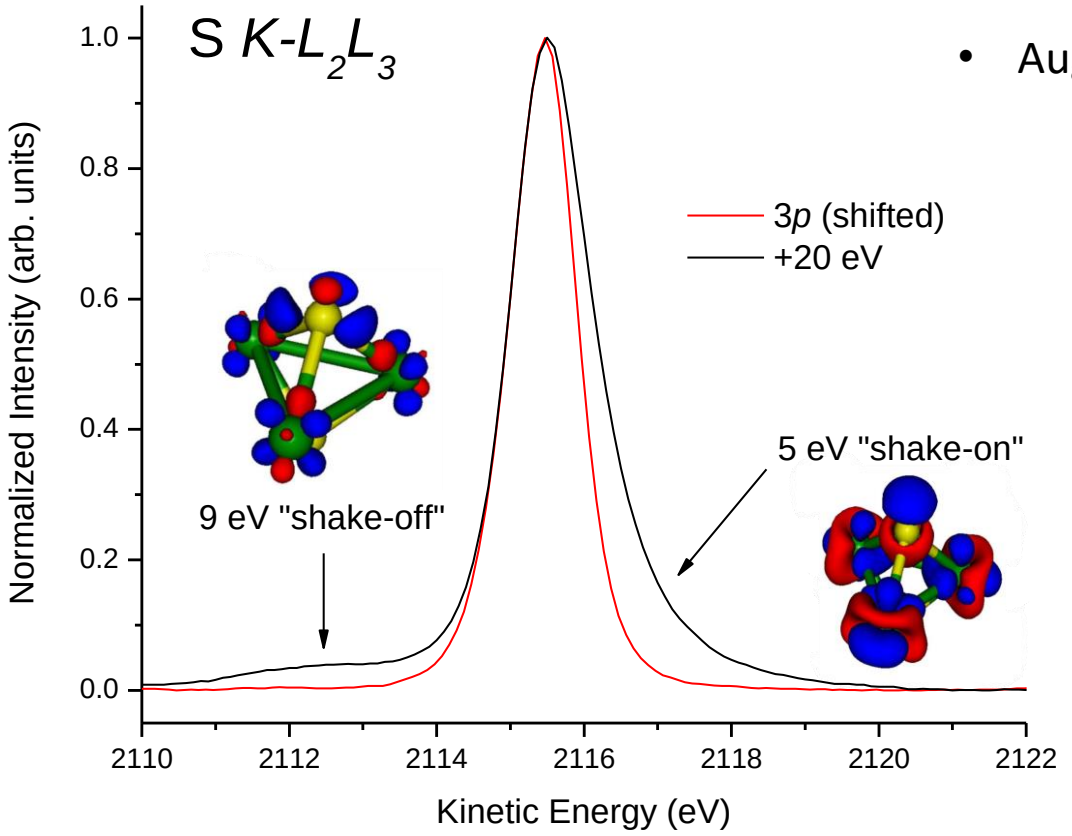

- Auger transition is *charge sensitive*…

Kinetic energy of Auger electron reveals **sign of charge transfer**!

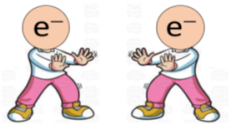

S *KLL* Auger MoS_2

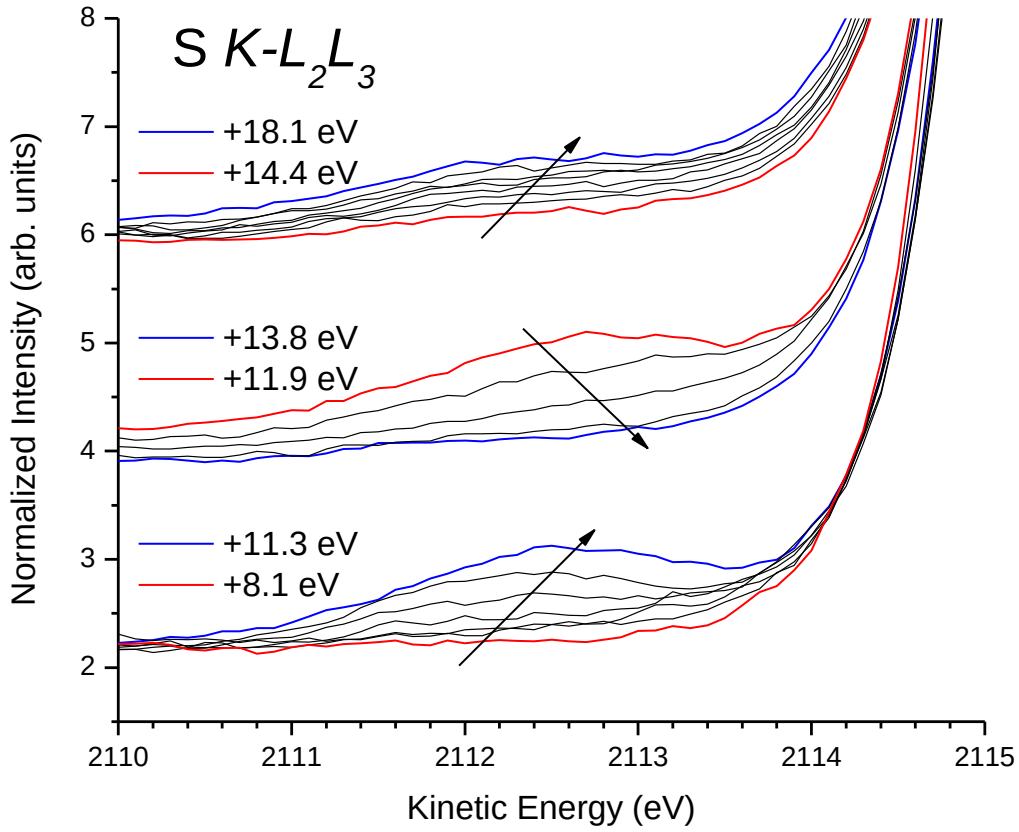

- Zoom in on low-energy Auger flank…

Decomposition of S *KLL* Auger peak: S 1*s* XAS

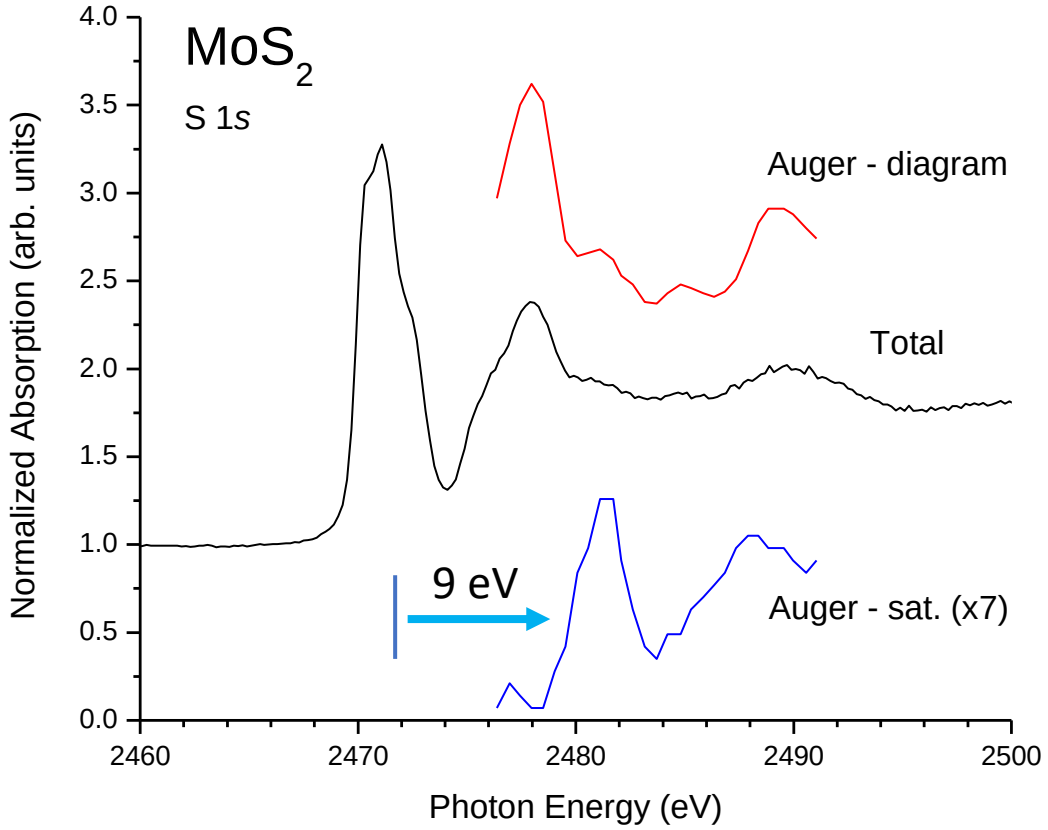

"The dipole sum rule states that the total absorption must remain the same independent of multielectron effects. The photo-electron can still have EXAFS associated with it, but the EXAFS will be ***shifted*** *to higher energy."*

E.A. Stern, B.A. Bunker, and S.M. Heald, *Phys. Rev. B* **21**, 5521 (1980).

LRO effects on NEXAFS

Woicik ~ 1986

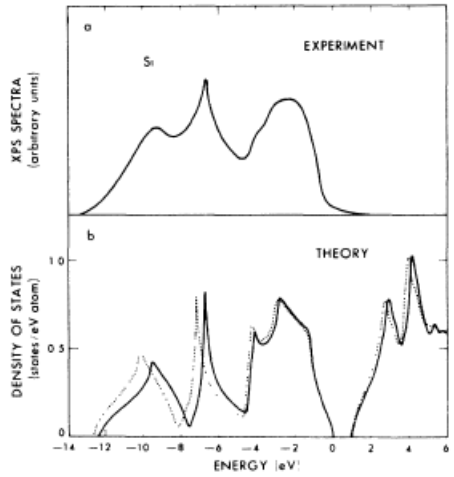

Chelikowski and Cohen, *PRB* (1974)

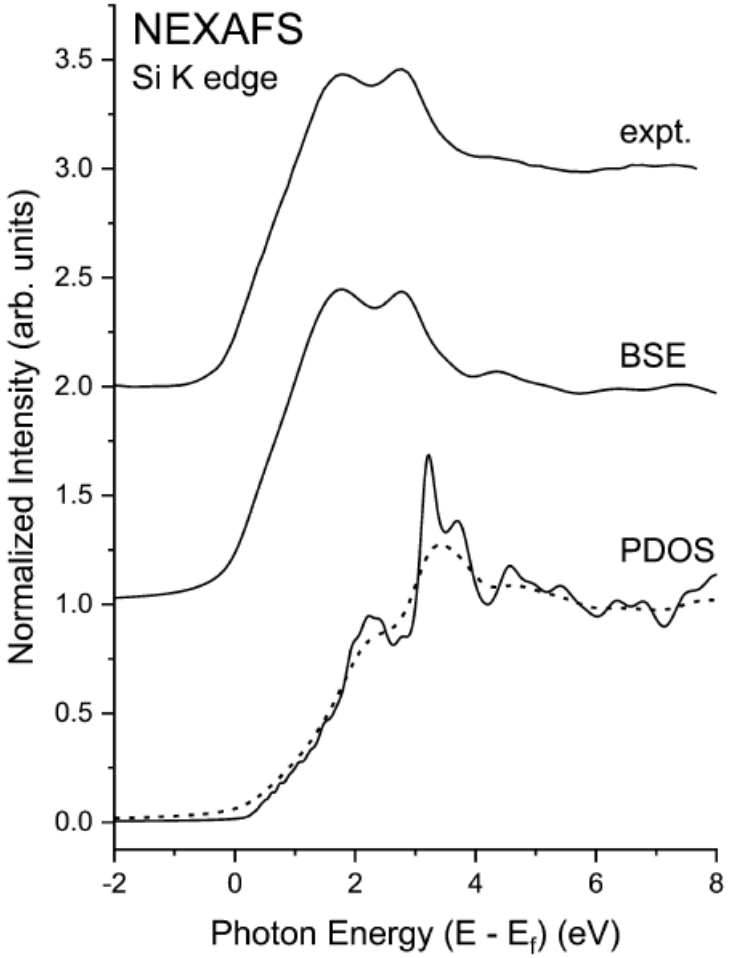

Shirley and Woicik, *PCCP* (2022)

Conclusions

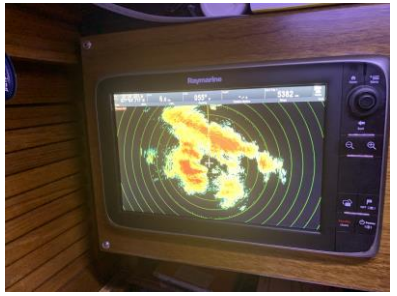

- ✓ Spectroscopy is a beautiful thing, the deeper you look the more you find…

- ✓ Congratulations on 50 years!